3. Applications in Statistical Physics

P.I. Hurtado

Departamento de Electromagnetismo y Física de la Materia, and Instituto Carlos I de Física Teórica y Computacional. Universidad de Granada. E-18071 Granada. Spain

E-mail: `phurtado@onsager.ugr.es`

Abstract. These notes correspond to the first part (20 hours) of a course on Computational Methods in Nonlinear Physics within the Master on Physics and Mathematics (*FisyMat*) of University of Granada. In this third chapter we focus on the application of Monte Carlo integration techniques in statistical physics, where the large number of degrees of freedom make Monte Carlo method a main tool.

Keywords: Computational physics, probability and statistics, Monte Carlo methods, stochastic differential equations, Langevin equation, Fokker-Planck equation, molecular dynamics.

References and sources

[1] R. Toral and P. Collet, *Stochastic Numerical Methods*, Wiley (2014).

[2] P.M. Chaikin and T.C. Lubensky, *Principles of Condensed Matter Physics*, Cambridge University Press (2003)

Contents

1. Introduction: Statistical mechanics and Monte Carlo methods

- One of the most important applications of the Monte Carlo sampling techniques appears in the field of statistical mechanics, which deals with systems with a large number of degrees of freedom N.

- A system is described by a set of coordinates $X = (x_1, \ldots, x_N)$. These variables x_i are typically positions, or angles, but more complicated examples of generalized coordinates exist in the literature. Each coordinate x_i has an associated conjugate momentum p_i and the whole set of X and $P = (p_1, \ldots, p_N)$ variables is required to fully specify the state of the system. We will denote by $\Gamma = (X, P)$ the combined set of $2N$ coordinate and momentum variables and a point in the Γ *phase space* as a *microscopic configuration*.

- Note that even the simplest macroscopic system will be described by an enormously large number of variables N. An order of magnitude of how large this number can be in typical situations is Avogadro's number $N_A = 6.022 \times 10^{23}$.

- An important function is the Hamiltonian $H(X, P) = H(x_1, \ldots, x_N, p_1, \ldots, p_N)$. It determines the time evolution of all $x_i(t)$ and $p_i(t)$, $i \in [1, N]$, via Hamilton's equations of motion

$$\frac{dx_i}{dt} = \frac{\partial H}{\partial p_i}, \tag{1}$$

$$\frac{dp_i}{dt} = -\frac{\partial H}{\partial x_i}, \tag{2}$$

All we need to do is to solve this set of $2N$ coupled first-order differential equations given some initial condition at, say, time $t = 0$. This is, of course, a tremendous (and impossible) task in most cases.

- The Hamiltonian can also be used to determine the probability density function of observing at thermal equilibrium some set of values for the coordinates and momenta $\Gamma = (X, P)$: that is, the probability of a

microscopic configuration. Boltzmann and Gibbs showed that such a pdf is given by what is nowadays called the Boltzmann factor, $\mathrm{e}^{-\beta H(\Gamma)}$, in the following manner:

$$f(\Gamma) = Z^{-1}\mathrm{e}^{-\beta H(\Gamma)} \,. \tag{3}$$

where

$$Z = \int d\Gamma \mathrm{e}^{-\beta H(\Gamma)} \tag{4}$$

is the normalization factor, $d\Gamma$ is the volume element in phase space, and $\beta = 1/kT$ is the inverse of the temperature rescaled by Boltzmann's constant k. Just not to hide anything, we can write this normalization factor in full, as

$$Z = \int dx_1 \ldots dx_n dp_1 \ldots dp_n \mathrm{e}^{-\beta H(x_1,\ldots,x_N,p_1,\ldots,p_N)} \,. \tag{5}$$

- In fact, this normalization factor by itself is very important, so important that it has a name, the *partition function*. The reason of its importance is that typical measures which can be determined experimentally concern the so-called thermodynamic potentials: Helmholtz's free energy F, internal energy U, enthalpy A, or the equation of state giving the pressure P as a function of volume V and temperature T, or the specific heat at constant volume C_V, or the isothermal compressibility κ_T, and so on. The framework of statistical mechanics tells us that all these quantities can be derived from the knowledge of the partition function as a function of only the volume V, the number of particles $\mathbf{N}$[1], and the temperature T. For example, Helmholtz's free energy is given by

$$F(\mathbf{N}, V, T) = -kT \log Z \,, \tag{6}$$

the internal energy is

$$U = \left(\frac{\partial(F/T)}{\partial(1/T)} \right)_{V,\mathbf{N}} \,, \tag{7}$$

† The number of particles $\mathbf{N}$ is not the same as the number of degrees of freedom N, as each particle can have, in general, more than one degree of freedom.

and the specific heat reads

$$C_V = \left(\frac{\partial U}{\partial T}\right)_{V,\mathbf{N}}.$$ (8)

The entropy can be computed from $S = (U - F)/T$ as

$$S = -\left(\frac{\partial F}{\partial T}\right)_{V,\mathbf{N}},$$ (9)

and so on.

- The *recipe* of statistical mechanics is extremely difficult to carry out in practice because the integrals involved in the definition of the partition function can only be performed for a limited number of simple examples: a gas of non-interacting particles, a system of independent harmonic oscillators, and so on, and a limited number of not-so-simple examples, the Gaussian free model and the Ising model for ferromagnetism being the most notable ones.

- Moreover, some interesting macroscopic observable phenomena only occur in the limit of the number of degrees of freedom N tending to infinity (as e.g. phase transitions), which makes the calculation of the partition function usually even harder.

- An alternative approach is to work not with the partition function directly but with the pdf of the microscopic configurations, $f(\Gamma)$. In this approach, some observables are defined in terms of averages with respect to this pdf. The average of any function of the microscopic variables $G(\Gamma)$ is defined in the usual way, as

$$\langle G \rangle = \int d\Gamma \, G(\Gamma) f(\Gamma).$$ (10)

- There are many examples. The internal energy can be computed as the average value of the Hamiltonian, $U = \langle H \rangle$. The specific heat C_V can also be obtained using higher order moments of the Hamiltonian as

$$C_V = k\beta^2 \left[\langle H^2 \rangle - \langle H \rangle^2 \right] , \tag{11}$$

and so on. Unfortunately, not all relevant magnitudes can be computed this way. For instance, the entropy S cannot be interpreted as the average value of some known function G[1].

- Many problems of statistical mechanics in equilibrium can then be reduced to the calculation of averages using the pdf $f(\Gamma) = Z^{-1} e^{-\beta H(\Gamma)}$. This probabilistic description (which lies at the core of statistical mechanics) is, in some cases, irrespective of whether the dynamical variables themselves satisfy Hamilton's equations.

- For instance, in problems of magnetism, a very successful approach consists in considering that the variables x_i represent microscopic magnetic moments that interact among themselves. In the simplest version, known as the Ising model, these microscopic variables can take only two possible values $x_i \equiv \mu s_i$, with μ being the unit of magnetic moment and $s_i = \pm 1$ is a rescaled variable (the Ising or spin variable). There are no momenta-like variables p_i associated with these magnetic moment variables and there are no Hamilton's equations. It does not even make sense to compute the time derivative of a noncontinuous variable s_i that can only take two possible values. Still, the microscopic variables s_i interact via the so-called Hamiltonian function $H(s_1, \ldots, s_N)$ and the probability of observing a particular configuration $\mathbf{s} = (s_1, \ldots, s_N)$ is $f(\mathbf{s}) = Z^{-1} e^{-\beta H(\mathbf{s})}$. The partition function now is not the integral over all values of s_i but, as s_i can take only two values $s_i = \pm 1$; it is computed as a sum

$$Z = \sum_{s_1 = \pm 1} \cdots \sum_{s_N = \pm 1} e^{-\beta H(s_1, \ldots, s_N)} . \tag{12}$$

† It is indeed possible to derive the formula $S = -\int d\Gamma f(\Gamma) \log[f(\Gamma)] + C$, with C a constant. Though formally this could be thought of as the average $S = -\langle \log f \rangle + C$, the truth is that, in order to perform this averaging, we must know the pdf $f(\Gamma)$, *including the normalization constant Z*, which is usually impossible. If we knew the partition function Z, we would not need any further integrals in order to compute the entropy; we would simply use Eqs. (6) and (9).

The Hamiltonian H takes into account the magnetic interactions, and it is typically simplified in order to consider only the interactions that occur between these Ising spins s_i which are close in space, neglecting the magnetic interactions with variables that are farther apart than some minimum cutoff distance. More details on this example later in this chapter.

- Once we have reduced the problem of equilibrium statistical mechanics to the calculation of averages, it is clear which should be an efficient numerical approach: replace the true average Eq. (10) by a sample average

$$\langle G \rangle = \mu[G] \pm \frac{\sigma[G]}{\sqrt{M}} \tag{13}$$

with

$$\mu[G] = \frac{1}{M} \sum_{k=1}^{M} G(\Gamma_k) \,, \tag{14}$$

$$\sigma^2[G] = \frac{1}{M} \sum_{k=1}^{M} G(\Gamma_k)^2 - (\mu[G])^2 \,, \tag{15}$$

with Γ_k, $k = 1, \ldots, M$, being the set of configurations generated stochastically. The key point is now the generation of characteristic configurations Γ_k distributed according to $f(\Gamma)$ in a problem with *many variables*. But this is precisely what we have claimed that Monte Carlo algorithms are good at! We now describe efficient rejection and dynamical methods to attack these kind of problems.

2. Dynamical methods in statistical physics

- In the dynamical methods, we proposed a change from a configuration Γ to a configuration Γ' taken from a pdf $g(\Gamma'|\Gamma)$. This proposal was then accepted with probability $h(\Gamma'|\Gamma)$.

- In order to ensure that the stationary distribution is $f(\Gamma)$, it is sufficient to demand that these conditional functions satisfy the detailed balance condition

$$g(\Gamma'|\Gamma)h(\Gamma'|\Gamma)f(\Gamma) = g(\Gamma|\Gamma')h(\Gamma|\Gamma')f(\Gamma') \tag{16}$$

  with $f(\Gamma) = Z^{-1}\mathrm{e}^{-\beta H(\Gamma)}$.

- A solution to this functional equation is given by the Metropolis algorithm, in which a proposal probability $g(\Gamma'|\Gamma)$ is first selected and then the acceptance probability is

$$h(\Gamma'|\Gamma) = \min\left[1, q(\Gamma'|\Gamma)\right] , \tag{17}$$

  where

$$q(\Gamma'|\Gamma) = \frac{g(\Gamma|\Gamma')f(\Gamma')}{g(\Gamma'|\Gamma)f(\Gamma)} . \tag{18}$$

- Most algorithms[1] assume that $g(\Gamma'|\Gamma)$ is a symmetric function, i.e. $g(\Gamma'|\Gamma) = g(\Gamma|\Gamma')$. In this case, and after replacing the expression for $f(\Gamma)$, we obtain

$$q(\Gamma'|\Gamma) = \frac{Z^{-1}\mathrm{e}^{-\beta H(\Gamma')}}{Z^{-1}\mathrm{e}^{-\beta H(\Gamma)}} = \mathrm{e}^{-\beta\Delta H} , \tag{19}$$

† But not all. A notable exception is the *hybrid Monte Carlo algorithm* explained in later chapters.

where $\Delta H = H(\Gamma') - H(\Gamma)$ is the change in energy in the proposal $\Gamma \to \Gamma'$. Note that the partition function Z disappears from the expression for $q(\Gamma'|\Gamma)$. The acceptance probability thus becomes

$$h(\Gamma'|\Gamma) = \min[1, e^{-\beta \Delta H}]. \tag{20}$$

This is the original proposal of the celebrated paper by Metropolis et al[1]

- It has an intuitive physical interpretation. The characteristic configurations at equilibrium are those that minimize Helmholt's free energy $F = U - TS$, a balance between the internal energy U (which tends to a minimum) and entropy S (which tends to a maximum). As $\Delta H \leq 0$ implies $h(\Gamma'|\Gamma) = 1$, this balance is achieved by (i) accepting all proposals $\Gamma \to \Gamma'$ in which the energy is reduced, and (ii) accepting those proposals in which energy increases $\Delta H > 0$ with a probability $e^{-\beta \Delta H}$. As $\beta = 1/kT$, when $T \to 0$ the probability of accepting a proposal that increases the energy tends to 0. On the contrary, when $T \to \infty$ (i.e. $\beta \to 0$), the acceptance probability tends to 1, and every proposal is accepted independently of the energy cost.

- Another solution to the detailed balance condition is that of Glauber:

$$h(\Gamma'|\Gamma) = \frac{q(\Gamma'|\Gamma)}{1 + q(\Gamma'|\Gamma)}, \tag{21}$$

or using that $q(\Gamma'|\Gamma) = e^{-\beta \Delta H}$,

$$h(\Gamma'|\Gamma) = \frac{1}{1 + e^{+\beta \Delta H}}, \tag{22}$$

Note that other choices for the acceptance probability h are still possible (van Beijeren and Schulman algorithm, heat bath method, etc.)

† Metropolis, N., Rosenbluth, A.W., Rosenbluth, M.N., Teller, A.H., and Teller, E., *Equations of state calculations by fast computing machine*, Journal of Chemical Physics **21**, 1087–1091 (1953).

3. Average acceptance probability and optimal configuration proposal

- To derive the average acceptance probability in the case of a pdf that is the exponential of a Hamiltonian, $f_{\hat{\mathbf{x}}}(\Gamma) = Z^{-1} e^{-\beta H(\Gamma)}$, we first need a helpful identity for the function $q(x|y)$ entering the acceptance probability. In particular, this identity is:

$$\langle q(y|x) \rangle_{\text{st}} = 1 \tag{23}$$

that holds in the stationary state. The averaging has to be performed with respect to the proposed values y (hence, distributed according to $g(y|x)$) over the allegedly stationary distribution of x. Namely

$$\langle q(y|x) \rangle_{\text{st}} = \int dy \int dx \, f_{\hat{\mathbf{x}}}(x) g(y|x) \, q(y|x) \,. \tag{24}$$

- The proof is simple, replace $q(y|x)$ by its definition $q(y|x) = \frac{g(x|y) f_{\hat{\mathbf{x}}}(y)}{g(y|x) f_{\hat{\mathbf{x}}}(x)}$ and manipulate

$$
\begin{aligned}
\langle q(y|x) \rangle_{\text{st}} &= \int dy \int dx \, f_{\hat{\mathbf{x}}}(x) g(y|x) \, q(y|x) = \int dy \int dx \, f_{\hat{\mathbf{x}}}(x) g(y|x) \frac{g(x|y) f_{\hat{\mathbf{x}}}(y)}{g(y|x) f_{\hat{\mathbf{x}}}(x)} \\
&= \int dy \left[\int dx \, g(x|y) \right] f_{\hat{\mathbf{x}}}(y) = \int dy f_{\hat{\mathbf{x}}}(y) = 1 \,.
\end{aligned} \tag{25}
$$

This should hold always in the stationary state.

- We now rewrite the previous result in order to derive the average acceptance probability in the case of a pdf that is the exponential of a Hamiltonian, $f_{\hat{\mathbf{x}}}(\Gamma) = Z^{-1} e^{-\beta H(\Gamma)}$, and assuming a symmetrical proposal $g(\Gamma|\Gamma') = g(\Gamma'|\Gamma)$

$$\langle q(\Gamma'|\Gamma) \rangle_{\text{st}} = \langle e^{-\beta \Delta H} \rangle_{\text{st}} = 1 \,, \tag{26}$$

where $\Delta H = H(\Gamma') - H(\Gamma)$ is the change in energy involved in the proposal $\Gamma \to \Gamma'$.

- If we use now Jensen's inequality $\langle e^{-z} \rangle \geq e^{-\langle z \rangle}$, which is valid for any random variable z, with $z = \beta \Delta H$, we derive that $e^{-\beta \langle \Delta H \rangle} \leq 1$, so in the steady state the average value of the proposed changes of energy is always greater or equal than zero, $\langle \Delta H \rangle \geq 0$.

- Although it is possible to be more general, we present here a simplified treatment which assumes that the distribution of the proposed changes of energy $z = \beta \Delta H$ can be well approximated by a Gaussian distribution of average μ and variance σ^2. For a Gaussian distribution we have $\langle e^{-z} \rangle = e^{-\mu + \sigma^2/2}$ and we have proved before that $\langle e^{-z} \rangle = 1$, we find that this Gaussian assumption is consistent if we take $\sigma^2 = 2\mu$.

- Let us now compute the average value of the Metropolis acceptance probability $h(\Gamma'|\Gamma) = \min[1, e^{-\beta \Delta H}]$ under the assumption that $z = \beta \Delta H$ follows a Gaussian distribution. We obtain for the average value

$$\langle h(\Gamma'|\Gamma) \rangle = \int_{-\infty}^{\infty} dz \, \min[1, e^{-z}] \frac{1}{\sqrt{2\pi\sigma^2}} e^{-(z-\mu)^2/2\sigma^2} . \tag{27}$$

Performing the integral and replacing $\sigma^2 = 2\mu$, we obtain the simple result

$$\langle h(\Gamma'|\Gamma) \rangle = \mathrm{erfc}\left(\frac{\sqrt{\mu}}{2}\right) = \mathrm{erfc}\left(\frac{\sqrt{\beta\langle \Delta H \rangle}}{2}\right) , \tag{28}$$

where $\mathrm{erfc}(z) = 1 - \mathrm{erf}(z)$ is the complementary error function.

- In the limit of large $\langle \Delta H \rangle$, we can use that $\mathrm{erfc}(z) \xrightarrow{z \to \infty} \frac{e^{-z^2}}{z\sqrt{\pi}}$ to obtain the asymptotic result

$$\langle h(\Gamma'|\Gamma) \rangle \xrightarrow{\langle \Delta H \rangle \to \infty} \frac{2 e^{-\beta\langle \Delta H \rangle/4}}{\sqrt{\pi\beta\langle \Delta H \rangle}} , \tag{29}$$

which shows that the average acceptance probability $\langle h(\Gamma'|\Gamma) \rangle$ goes to zero exponentially with the average (positive) energy change $\langle \Delta H \rangle$.

- As H is usually an extensive quantity proportional to the number of degrees of freedom N, it is important to devise proposals in which the change of energy ΔH can be kept small, $O(1)$ instead of $O(N)$; otherwise, the small average acceptance probability will yield a very large correlation time and the corresponding large statistical errors will make the estimator useless.

- The standard trick to keep a reasonable acceptance probability is to propose new configurations Γ' in which only a few degrees of freedom have been modified from configuration Γ.

- Collective updates in which all degrees of freedom change at once but still the acceptance probability is nonvanishingly small are much more difficult to devise. We will devote a later chapter to explain some collective update algorithms, and restrict ourselves in the rest of this chapter to algorithms in which the proposal involves the change of a few (maybe only one) variable.

4. Interacting particles

- The first case we will consider is that of interacting particles without internal degrees of freedom. This means that all we need to specify the state are the spatial locations $\boldsymbol{r}_i$ of the $i = 1, \ldots, \mathbf{N}$ particles, as well as the associated momenta $\boldsymbol{p}_i = m\boldsymbol{v}_i$, with m being the mass of the particle (assumed identical) and $\boldsymbol{v}_i$ the velocity.

- In general, $\boldsymbol{r}_i = (x_i, y_i, z_i)$ and $\boldsymbol{p}_i = (p_i^x, p_i^y, p_i^z)$ are three-dimensional vectors, although other spatial dimensions can be considered in specific cases. We can think of the particles as perfect spheres (or rods in one dimension and disks in two dimensions) moving around while interacting with other particles.

- The Hamiltonian consists of two terms, corresponding to the kinetic ($\mathcal{T}$) and potential ($\mathcal{V}$) energy. In the potential energy, we must consider interactions between all possible pairs of particles (i, j) which, following convention, we order using $i < j$. As the particles have no internal degrees of freedom, the potential interaction $V(\boldsymbol{r}_i, \boldsymbol{r}_j)$ between particles i and j depends only on the location of the particles (we assume it does not depend on their velocities). The Hamiltonian is, then

$$H(\boldsymbol{r}_1, \ldots, \boldsymbol{r}_\mathbf{N}, \boldsymbol{p}_1, \ldots, \boldsymbol{p}_\mathbf{N}) = \mathcal{T}(\boldsymbol{p}_1, \ldots, \boldsymbol{p}_\mathbf{N}) + \mathcal{V}(\boldsymbol{r}_1, \ldots, \boldsymbol{r}_\mathbf{N}) \tag{30}$$

with

$$\mathcal{T}(\boldsymbol{p}_1, \ldots, \boldsymbol{p}_\mathbf{N}) = \sum_{i=1}^{\mathbf{N}} \frac{\boldsymbol{p}_i^2}{2m} \qquad ; \qquad \mathcal{V}(\boldsymbol{r}_1, \ldots, \boldsymbol{r}_\mathbf{N}) = \sum_{i<j} V(\boldsymbol{r}_i, \boldsymbol{r}_j) \tag{31}$$

- We see that the equilibrium, Maxwell-Boltzmann pdf $e^{-\beta H}$ can be split naturally as

$$e^{-\beta H} = \left[\prod_{i=1}^{\mathbf{N}} e^{-\beta \boldsymbol{p}_i^2/2m} \right] \times e^{-\beta \sum_{i<j} V(\boldsymbol{r}_i, \boldsymbol{r}_j)} = \left[\prod_{i=1}^{\mathbf{N}} e^{-\beta(p_i^x)^2/2m} e^{-\beta(p_i^y)^2/2m} e^{-\beta(p_i^z)^2/2m} \right] \times e^{-\beta \sum_{i<j} V(\boldsymbol{r}_i, \boldsymbol{r}_j)} \tag{32}$$

which indicates that, from the statistical point of view, each one of the momentum coordinates (p_i^x, p_i^y, p_i^z) is independently distributed with a Gaussian distribution of zero mean and variance $m/\beta = kTm$. This independence allows us to obtain analytically some averages of interest.

- For instance, the average value of the kinetic energy is

$$\left\langle \sum_{i=1}^{\mathbf{N}} \frac{\boldsymbol{p}_i^2}{2m} \right\rangle = \frac{3}{2}\mathbf{N}kT \tag{33}$$

  as each of the $3\mathbf{N}$ Gaussian variables contributes a factor $kT/2$ (energy equipartition theorem).

- On the other hand, averages of functions $G(\boldsymbol{r}_1, \ldots, \boldsymbol{r_N})$ which depend on the coordinates, are much more difficult to perform analytically because of the interaction terms. Here is where the numerical methods here explained are useful. The formal expression is

$$\langle G(\boldsymbol{r}_1, \ldots, \boldsymbol{r_N}) \rangle = C^{-1} \int d\boldsymbol{r}_1 \ldots d\boldsymbol{r_N} G(\boldsymbol{r}_1, \ldots, \boldsymbol{r_N}) \, e^{-\beta \mathcal{V}(\boldsymbol{r}_1, \ldots, \boldsymbol{r_N})}, \tag{34}$$

  i.e. an average with respect to the pdf

$$f(\boldsymbol{r}_1, \ldots, \boldsymbol{r_N}) = C^{-1} e^{-\beta \mathcal{V}(\boldsymbol{r}_1, \ldots, \boldsymbol{r_N})} \tag{35}$$

  with $C = \int d\boldsymbol{r}_1 \ldots d\boldsymbol{r_N} \, e^{-\beta \mathcal{V}(\boldsymbol{r}_1, \ldots, \boldsymbol{r_N})}$ the normalization constant.

- To perform these averages numerically, we generate configurations of positions $X = (\boldsymbol{r}_1, \ldots, \boldsymbol{r_N})$ distributed according to this pdf and approximate the average in Eq. (34) by the sample average, including an estimation of the error.

- In order to generate the configurations, we can use, for example, the Metropolis algorithm, in which we propose a change from $X \to X'$ according to some distribution $g(X'|X)$. We have much freedom in choosing the new configuration X', but we must do so such that the resulting acceptance probability $h(X'|X)$ is not vanishingly small.

- As explained earlier, we choose a proposal X' that differs from X in just a few variables. For instance, we can choose, most naturally, to change the position $\boldsymbol{r}_i \to \boldsymbol{r}'_i$ of a single particle, randomly chosen among the particles. In this way, $g(X'|X)$ is constructed from $g(\boldsymbol{r}'_i|\boldsymbol{r}_i)$, which depends only on the coordinates of the randomly chosen particle i.

- We can choose, for instance (but we stress that we have a lot of freedom in this proposal step), to change every Cartesian coordinate $(x_i, y_i, z_i) \to (x'_i, y'_i, z'_i)$ such that x'_i, y'_i and z'_i are drawn from a uniform distribution in the intervals $(x_i - \Delta, x_i + \Delta)$, $(y_i - \Delta, y_i + \Delta)$ and $(z_i - \Delta, z_i + \Delta)$, respectively. As this proposal is symmetrical, $g(X'|X) = g(X|X')$, the detailed balance condition reads now

$$h(X'|X)\mathrm{e}^{-\beta \mathcal{V}(X)} = h(X|X')\mathrm{e}^{-\beta \mathcal{V}(X')} \tag{36}$$

in terms of the potential energy $\mathcal{V}$ only. We can take, for instance, the Metropolis solution

$$h(X'|X) = \min \left[1, \mathrm{e}^{-\beta \Delta \mathcal{V}} \right] \tag{37}$$

where $\Delta \mathcal{V} = \mathcal{V}(X') - \mathcal{V}(X)$ is the change in the potential energy induced by the proposed change $X \to X'$. As only the position $\boldsymbol{r}_i$ is modified, the change is

$$\Delta \mathcal{V} = \sum_{j \neq i} \left[V(\boldsymbol{r}'_i, \boldsymbol{r}_j) - V(\boldsymbol{r}_i, \boldsymbol{r}_j) \right] . \tag{38}$$

- Usually, the interaction potential depends on the separation distance $r_{ij} = |\boldsymbol{r}_i - \boldsymbol{r}_j|$ between particles i and j, i.e. $V(\boldsymbol{r}_i, \boldsymbol{r}_j) = V(r_{ij})$. This is the case, for example, of the celebrated Lennard-Jones (or 6-12) potential

$$\mathcal{V}(r) = V_0 \left[\left(\frac{r_0}{r} \right)^{12} - \left(\frac{r_0}{r} \right)^{6} \right] , \tag{39}$$

where V_0 and r_0 are the parameters of the potential.

- Note that in this case, and for a large number of particles, the calculation of the sum (41) can be very expensive from the computational point of view because a sum of terms must be calculated every time a single position is proposed to change. This is another reason why collective update proposals, in which all variables $(\boldsymbol{r}_1, \ldots, \boldsymbol{r_N})$ are proposed to change simultaneously, are more effective. A particular type of collective updating suitable for this kind of systems and known as the hybrid Monte Carlo will be explained in later chapters.

- Another solution to limit the computational cost of the sum (41) is to introduce a cutoff distance R beyond which the potential is small enough so it can be truncated to zero. For the Lennard-Jones potential, this is typically implemented as follows

$$\mathcal{V}(r) = \begin{cases} V_0 \left[\left(\frac{r_0}{r}\right)^{12} - \left(\frac{r_0}{r}\right)^6 \right], & r \le R\,, \\ 0\,, & r > R\,. \end{cases} \tag{40}$$

In this case, the sum (41) has a much smaller number of terms:

$$\Delta\mathcal{V} = \sum_{j, |\boldsymbol{r}'_i - \boldsymbol{r}_j| < R, |\boldsymbol{r}_i - \boldsymbol{r}_j| < R} \left[V(\boldsymbol{r}'_i, \boldsymbol{r}_j) - V(\boldsymbol{r}_i, \boldsymbol{r}_j) \right]\,. \tag{41}$$

However, some nontrivial bookkeeping (in the form of neighbor lists) is necessary in order to keep track of which particles j are at a distance less than the cutoff from the particle i whose position is proposed to change to $\boldsymbol{r}'_i$.

- The main features of the Lennard-Jones potential are the presence of a repulsion term (r^{-12}) at short distances and an attraction, Van der Waals term (r^{-6}) decreasing to zero at long distances. These features can be captured by simpler models. For instance, the potential

$$\mathcal{V}(r) = \begin{cases} \infty\,, & r \le 2\sigma\,, \\ -V_0\,, & 2\sigma < r \le R\,, \\ 0\,, & r > R\,. \end{cases} \tag{42}$$

signifies that the attraction between particles occurs only if they are closer than a distance R and that the repulsion energy is infinite if particles try to get closer than a distance 2σ, modeling the so-called hard-core repulsion. This can be imagined as each particle being a sphere of radius σ, such that the energetic cost of bringing two particles closer than a distance of one diameter, 2σ, is infinite.

- When only the repulsion term is taken into consideration, that is, when the potential is

$$\mathcal{V}(r) = \begin{cases} \infty, & r \le 2\sigma, \\ 0, & r > 2\sigma. \end{cases} \tag{43}$$

we talk about a system of hard spheres. $\Delta \mathcal{V}$ is either zero, if the new position $\boldsymbol{r}_i'$ is such that the particle does not overlap with any other, or infinite, in case there is one particle j with which it overlaps. The acceptance probability is, hence

$$h(X'|X) = \min[1, \mathrm{e}^{-\beta \Delta \mathcal{V}}] = \begin{cases} 0, & \text{if exists } j \text{ such that } |\boldsymbol{r}_i' - \boldsymbol{r}_j| < 2\sigma, \\ 1, & \text{otherwise}. \end{cases} \tag{44}$$

In other words, movements are accepted if and only if they do not lead to overlaps between particles.

- Again, the program can be made much more efficient by making an a priori list containing the particles with which particle i can overlap after it is moved.

- Simple as it might look, the system of hard spheres has been extensively studied both from the theoretical and numerical points of view.

5. The Ising model

- Although it has been used in very different contexts (from phase separation in binary metal alloys to segregation in urban communities), its most direct application (and the one it was originally introduced for) is as a model for magnetic materials.

- Imagine a substance displaying a paramagnetic to ferromagnetic transition. This is to say, the magnet loses its spontaneous magnetization at high temperatures (above the so-called Curie temperature)[1]. We can simplify the complicated structure of the magnetic solid by a perfect, regular lattice and assume that in every site i of this lattice lies a microscopic magnet that is capable of taking two possible values $x_i = \mu s_i = \pm \mu$ for the magnetic moment.

- Here, s_i is called the *spin* variable (a name reflecting the fact that the magnetism has its origin in the individual atomic spins). The value $s_i = +1$ means that the local magnetic moment points upward in an arbitrary, Z, direction, while a value $s_i = -1$ indicates that the local magnetic moment points downward in the opposite direction. A microscopic configuration $\boldsymbol{s} = (s_1, \ldots, s_N)$ is a set of values for the N spin variables.

- The last ingredient is an energy function, which is a Hamiltonian[2] reflecting the magnetic interaction between the spins. In ferromagnetic materials, the interaction is such that it favors two spins to point in the same direction. This is reflected in a potential interaction $-J_{ij}\, s_i s_j$ between the spins at sites i and j, with J_{ij} the coupling (or exchange) constant between sites i and j, a positive parameter, $J_{ij} > 0$. Hence, if s_i and s_j are both parallel, i.e. both take the value +1 or the value -1, then the interaction energy is $-J_{ij} < 0$, whereas if they are antiparallel, one of them +1 and the other -1, the interaction energy is $+J_{ij} > 0$, which is higher (for $J_{ij} > 0$) than in the case of parallel alignments.

† We might not be very familiar with this situation, as the most common magnetic material, iron, loses its magnetization at around 770°C, certainly not a temperature we come across every day.
‡ We stress however that there are no Hamilton's equations of motion associated with this function.
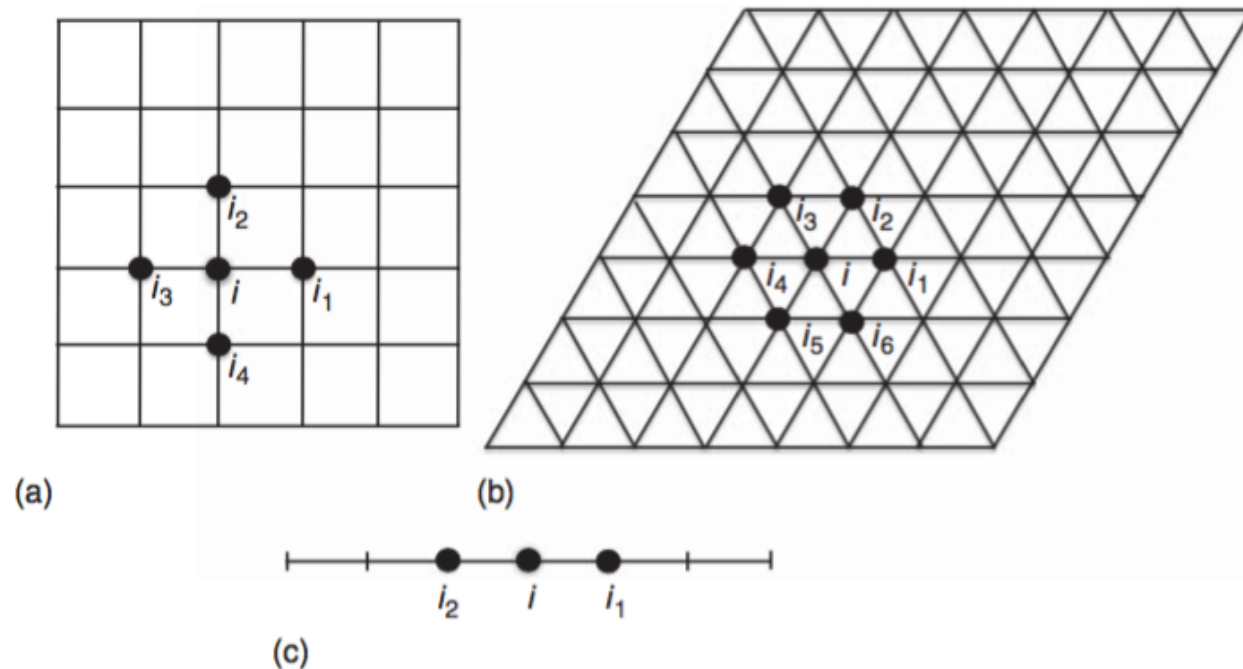
Figure 1. Some common lattices and the structure of their nearest neighbors. (a) In a square lattice, node i has four nearest neighbors: i_1, i_2, i_3 and i_4. (b) In a triangular lattice, node i has six nearest neighbors: i_1, i_2, i_3, i_4, i_5 and i_6. (c) In a linear chain, node i has two nearest neighbors: i_1 and i_2.

- The exchange interaction energy J_{ij} decays with the distance between the sites i and j. An important simplification of the model is to assume that the interaction is very short-ranged and occurs only for those spins that are sufficiently close in the regular lattice. What is meant by *"sufficiently close"* depends on the type of lattice, but usually one adopts the point of view that only those spins that lie separated by the minimum distance dictated by the lattice are capable of interacting between them. Those spins are then said to be the *nearest neighbors* in the lattice, and their exchange constant is then $J_{ij} = J$. In Figure 1, we plot some common lattices and the underlying structure of the nearest neighbors.

- The Hamiltonian also considers the possible existence of a magnetic field h with which spins tend to align. This is reflected by a term $-h\,s_i$ which takes its minimum value whenever the signs of h and s_i coincide.

- With all these considerations in mind, the Hamiltonian of the Ising model is

$$H(s_1, \ldots, s_N) = -J \sum_{\langle i,j \rangle} s_i\, s_j - h \sum_i s_i\,, \tag{45}$$

  where the notation $\langle i, j \rangle$ indicates all the pairs of sites i, j that are nearest neighbors in the chosen lattice.

- The basic phenomenology of the Ising model in the absence of a magnetic field, $h = 0$, is that the tendency to align parallel dominates at low temperatures and there is a vast majority of spins pointing in the same direction, a situation identified with macroscopic order. Whether this direction is up, $s_i = +1$, or down, $s_i = -1$, depends on many things (e.g., the initial conditions). The choice of one of the two, which are otherwise equivalent, directions is an example of *symmetry breaking*.

- At temperatures above a critical value, T_c, the disordering role dominates and approximately half of the spins point upward and half downward. The symmetry has been restored. This competition between an ordering agent (the coupling constant) and a disordering one (the temperature) and the resulting transition between order and disorder is arguably the simplest example of a *phase transition*, the phases being the ordered state at low temperatures (the ferromagnetic phase) and the disordered state at high temperatures (the paramagnetic phase). This competition between ordering and disordering agents and the resulting phase transition phenomenon can be found in many situations, not only in physical systems, and the Ising model is then used as a paradigmatic case study.

5.1. Mean field (Bragg-Williams) theory for the Ising model

- Mean-field theory is an approximation for the thermodynamic properties of a system based on treating the order parameter as spatially constant. It is a useful description if spatial fluctuations are not important. It becomes an exact theory only when the range of interactions becomes infinite. It, nevertheless, makes quantitatively correct predictions about some aspects of phase transitions (e.g. critical exponents) in high spatial dimensions where each particle or spin has many nearest neighbors, and it makes *qualitatively* correct predictions in physical dimensions. Mean-field theory has the enormous advantage of being mathematically simple, and it is almost invariably the first approach taken to predict phase diagrams and properties of new experimental systems.

- There are many formulations of mean-field theory, beginning with the van der Waals equation of state (1873) for the liquid-gas transition and the Weiss molecular field theory for ferromagnetism. In this subsection, we will introduce mean-field Bragg-Williams theory for an Ising ferromagnet (WL. Bragg and EJ. Williams, 1934). This theory is equivalent to the Weiss molecular field theory and provides a qualitatively correct description of the properties of the Ising model at all temperatures, including the vicinity of zero temperature.

- The free energy F is the difference between the internal energy, $E = \langle H \rangle$, and $T S$, the temperature times the entropy,

$$F = E - T S \,. \tag{46}$$

  Thus, F can be obtained if E and TS can be calculated separately as a function of the order parameter. In the Ising model, the order parameter $m = \langle s \rangle$ is the average of the spin.

- The entropy for a given spatially uniform m can be calculated exactly. The total magnetic moment is simply the number N_+ of up spins minus the number N_- of down spins, and

$$m = \frac{1}{N} \sum_{i=1}^{N} s_i = \frac{N_+ - N_-}{N} \,, \tag{47}$$

where $N = N_+ + N_-$ is the total number of sites in the lattice. The entropy for a given m, following Boltzmann's celebrated formula, is the logarithm of the number of configurations with a given m, or equivalently, with a fixed N_+ (as $N_- = N - N_+$), so

$$S = \ln \binom{N}{N_+} = \ln \binom{N}{N(1+m)/2} = \ln \left[\frac{N!}{(N(1+m)/2)! \, N(1-m)/2!} \right] , \tag{48}$$

$$\frac{S}{N} \equiv s(m) = \ln 2 - \frac{1}{2}(1+m)\ln(1+m) - \frac{1}{2}(1-m)\ln(1-m) , \tag{49}$$

where we have used Stirling approximation $n! \approx n^n e^{-n} \sqrt{2\pi n}$ since N is very large. This entropy is often called the entropy of mixing.

- To evaluate E, one should calculate $\langle H \rangle = Z_m^{-1} \int d\Gamma(m) H[\Gamma(m)] e^{-\beta H[\Gamma(m)]}$, where $\int d\Gamma(m)$ is an integral over all configurations Γ with fixed m and $Z_m = \int d\Gamma(m) e^{-\beta H[\Gamma(m)]}$. An exact evaluation of this average would constitute an exact solution of the Ising model and is quite complicated. In Bragg-Williams theory, $\langle H \rangle$ is approximated by replacing s_i in H by its position independent average m:

$$E = -J \sum_{\langle i,j \rangle} m^2 = -\frac{1}{2} J N z m^2 , \tag{50}$$

where z is the coordination number, or the number of nearest neighbor sites in the lattice ($z = 2d$ for a d-dimensional hypercubic lattice). (Recall that $\langle i, j \rangle$ signifies the bond between nearest neighbors i and j.)

- The complete Bragg-Williams free energy is thus

$$f(T,m) = \frac{1}{N}(E - TS) = -\frac{1}{2}Jzm^2 + \frac{1}{2}T\left[(1+m)\ln(1+m) - \frac{1}{2}(1-m)\ln(1-m)\right] - T\ln 2 \tag{51}$$
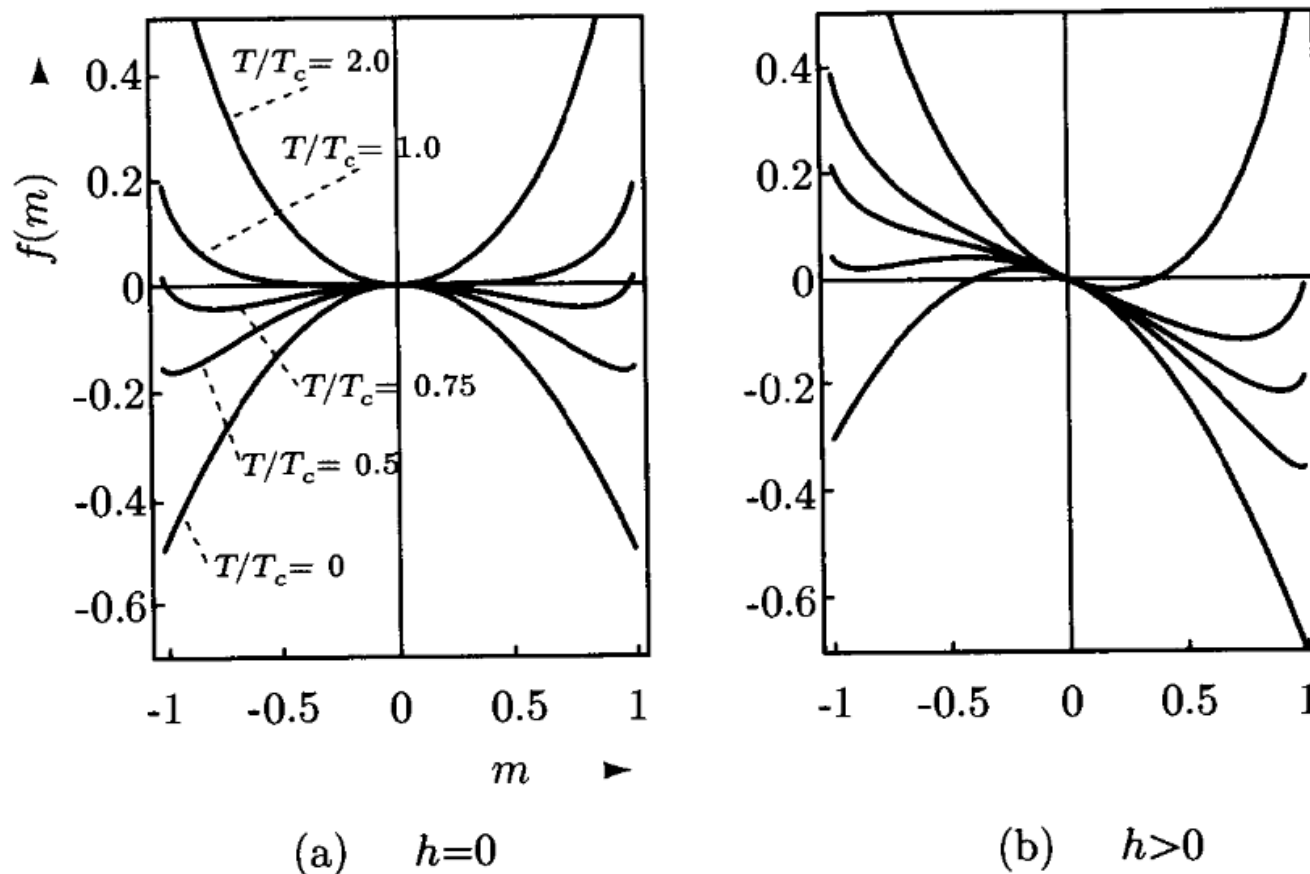
Figure 2. (a) The Bragg-Williams free energy as a function of order parameter for various values of T/T_c. For $T > T_c$, there is a single minimum at $m = 0$. At $T = T_c$, the single minimum at $m = 0$ is very broad. For $T < T_c$, there are two minima with the same free energy at $\pm m$. At $T = 0$, the minimum of the free energy occurs at $m = \pm 1$. (b) The Bragg-Williams free energy $f(m,T) - hm$ in an external magnetic field of $h = 0.2T_c > 0$. Note that the minimum at $T > T_c$ occurs at positive m. The minimum at positive m for $T < T_c$ has a lower free energy than that at negative m (metastable state). The order parameter m is restricted to lie between 0 and 1. At $T = 0$, the absolute minimum of the free energy occurs at $m = +1$ when $h = 0$. The derivative $\partial f/\partial m$ is, however, not zero at these minima. For $T > 0$, $\partial f/\partial m$ is zero at the absolute minimum of f, which occurs at $|m| < 1$.

- This free energy function is plotted for various values of T in Fig. 2. Note that it is even under the operation $m \to -m$; it could, therefore, be expressed as a function of m^2 rather than m. For large T, $f(m)$ has a single minimum at $m = 0$. Below a critical temperature T_c (to be calculated below), it has two minima at $\pm m$. As $T \to 0$, the two minima occur at values of $|m|$ closer and closer to unity.

- In the absence of an external aligning magnetic field h, the equilibrium value of $m(T)$ is the one which minimizes $f(m, T)$ at fixed T. Thus, the disappearance of the minimum at $m = 0$ and the emergence of lower free energy minima at nonzero m corresponds to a phase transition. As we shall see shortly, the value of m at the new minima grows continuously from zero, so the transition is second order.

- In the vicinity of T_c where m is small, we can expand $s(m)$ and $f(m)$ in powers of m:

$$s(m) = \ln 2 - \frac{1}{2}m^2 - \frac{1}{12}m^4 + \dots , \qquad (52)$$

so that

$$f(m) = \frac{1}{2}(T - T_c)m^2 + \frac{1}{12}Tm^4 - T\ln 2 + \dots , \qquad (53)$$

where $T_c = zJ$ is the mean-field transition temperature. For $T > T_c$, $f(m)$ has a positive curvature at the minimum at the origin, while for $T < T_c$ it has negative curvature at the maximum at the origin and positive curvature at the minima at nonzero m.

- In the presence of a positive external field h, the function $f(m) - hm$ is asymmetric with a single minimum for $T > T_c$ with $m > 0$, as shown in Fig. 2.b. When $T < T_c$, there are two minima in $f(m) - hm$. The minimum with $m > 0$ is the absolute minimum and corresponds to the equilibrium state. The relative minimum with $m < 0$ is a metastable state, where the system may get trapped for a long time, eventually relaxing to the true stable state at $m > 0$.

- The equation of state in an external field, i.e. the system magnetization as a function of T and h, is obtained by solving for m the equation $\partial(f - hm)/\partial m = 0$, or equivalently

$$\frac{\partial f}{\partial m} = -zJm + \frac{1}{2}T \ln \left[\frac{1+m}{1-m}\right] = h = -zJm + T \tanh^{-1} m \,. \tag{54}$$

Thus,

$$m = \tanh \left[\frac{h + T_c m}{T}\right] \,. \tag{55}$$

The quantity $h_m \equiv h + T_c m$ is the average local or mean field at a given site. It arises both from the external field and from the exchange field produced by the neighboring spins with average spin m. The actual local field at a given site depends on the local configurations of spins on neighboring sites. The quantity $zJm = T_c m$ is the average or mean field arising from neighboring sites.

- The solutions to Eq. (55) are best visualized graphically, as shown in Fig. 3. When $h = 0$, the slope T_c/T of $\tanh(T_c m/T)$ at $m = 0$ is less than one for $T > T_c$ and greater than one for $T < T_c$. Thus for $T > T_c$, the only solution to Eq. (55) with $h = 0$ is $m = 0$. For $T < T_c$, there are three solutions, $\pm m(T)$ and zero. The tanh function lies between -1 and +1 so that $|m| < 1$. As $T \to 0$, $\tanh(T_c m/T)$ saturates at its maximum values of one at smaller and smaller m, and $|m(T)| \to 1$ as $T \to 0$ indicating full ferromagnetic order as expected in the fully aligned ground state of the Ising model. Indeed, near $T = 0$ we have

$$m = \tanh(T_c m/T) \approx 1 - 2e^{-2zJ/T} \tag{56}$$

so that m tends to unity exponentially with temperature.

- As $T \to T_c^-$, the solution to Eq. (55) can be obtained by expanding $\tanh x$ in powers of x, i.e. $\tanh x \approx x - \frac{1}{3}x^3$, so

$$m \approx \frac{T_c}{T}m - \frac{1}{3}\left(\frac{T_c}{T}\right)^3 m^3 \approx \frac{T_c}{T}m - \frac{1}{3}m^3 \tag{57}$$
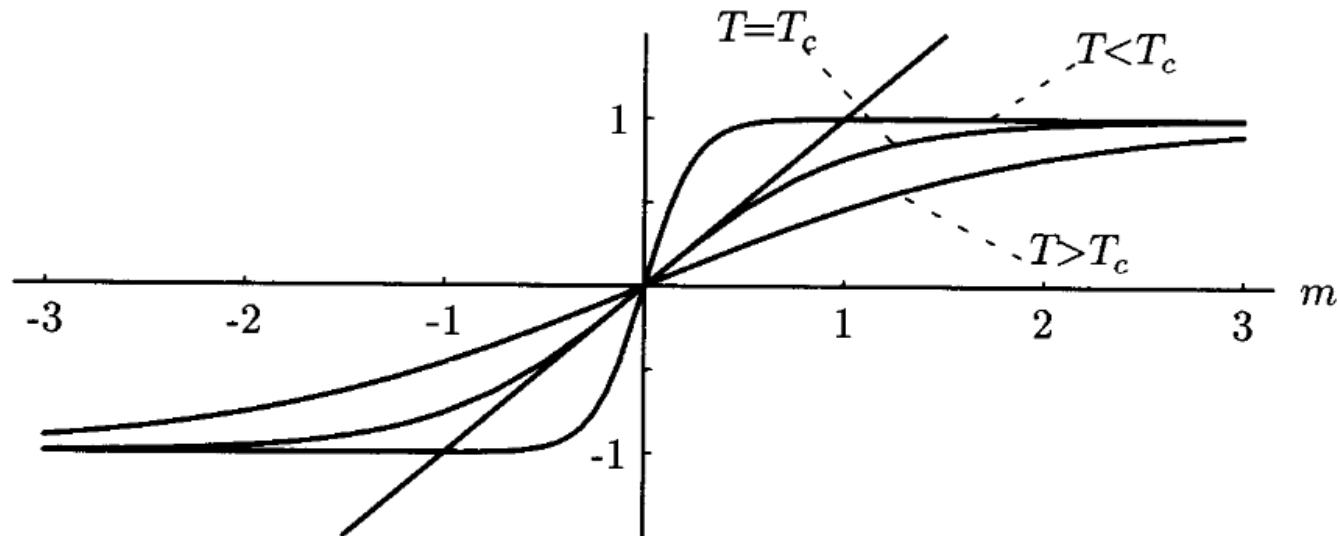
Figure 3. Graphical solution of the Ising mean-field equation of state, Eq. (55), for $h = 0$. For $T > T_c$, the linear function m intersects the tanh function only at the origin. For $T < T_c$, the slope of $\tanh(T_c m/T)$ at the origin is greater than one, and there are three solutions to the equation of state corresponding to the two minima and one maximum (at the origin) of the free energy.

or

$$m = \pm \left[\frac{3(T_c - T)}{T} \right]^{1/2} . \tag{58}$$

Thus m tends continuously to zero as $(T_c - T)^{1/2}$. This behavior is a general feature of second order mean-field phase transitions.

- The Bragg-Williams free energy can be used to calculate other thermodynamic quantities such as the internal energy and entropy and their derivatives.

- Mean field theory is just an approximation, and real life is far more complex. The spontaneous magnetization (i.e. the magnetization at zero magnetic field, $m(T, 0) \equiv m_0(T)$) of a system of interacting spins *might* be non-zero for temperatures below a critical one, but detailed calculations for the Ising model show that this behavior is observed *depending on the dimension*.

- For one-dimensional ($1d$) lattices in which spins have only two nearest neighbors, which is the case considered by Ising himself, the spontaneous magnetization is always zero, independent of temperature. However, the generic behavior for lattices in two or more dimensions is the existence of a critical temperature below which the spontaneous magnetization is indeed different from zero.

- From the analytical point of view, only a limited set of lattices can be studied, including a variety of two-dimensional lattices and the fully connected lattice in which every spin is connected to every other spin. It is worth mentioning here the work by Lars Onsager who in an authentic mathematical tour de force was able to compute the free energy and the related thermodynamic potential in the case of zero magnetic field for the regular square lattice. He was also able to find the spontaneous magnetization. Despite the tremendous difficulty of the calculation, the spontaneous magnetization is given by a deceptively simple expression

$$m_0(T) = \begin{cases} (1 - [\sinh(2J/kT)]^{-4})^{1/8} \,, & T \leq T_c \\ 0 \,, & T > T_c \,, \end{cases} \tag{59}$$

with a value of the critical temperature $T_c/J = 2/\ln(1 + \sqrt{2}) \approx 2.2691853\ldots$

5.2. Monte Carlo simulation of the Ising model: Metropolis algorithm

- An alternative to the complicated analytical calculations described above is the use of the Monte Carlo method to sample the equilibrium distribution of the Ising model.

- Which averages of functions G of the spin variables $\boldsymbol{s} = (s_1, \ldots, s_N)$ are useful to compute in the Ising model? Without any doubt, the most important one is the magnetization per particle, defined as

$$m = \left| \frac{1}{N} \sum_{i=1}^{N} s_i \right|,\tag{60}$$

  and its ensemble average $\langle m \rangle$.

- Averages of any function $G(\boldsymbol{s})$ are performed using the Boltzmann factor $\mathrm{e}^{-\beta H(\boldsymbol{s})}$, or

$$\langle G \rangle = \frac{\displaystyle\sum_{s_1=\pm 1} \cdots \sum_{s_N=\pm 1} G(s_1, \ldots, s_N)\mathrm{e}^{-\beta H(\boldsymbol{s})}}{\displaystyle\sum_{s_1=\pm 1} \cdots \sum_{s_N=\pm 1} \mathrm{e}^{-\beta H(\boldsymbol{s})}}.\tag{61}$$

- Other important quantities are the magnetic susceptibility $\chi_T = \left.\frac{\partial m(T,h)}{\partial h}\right|_{h=0}$, which can be related to fluctuations of the order parameter m

$$\chi_T = \frac{N}{kT}\sigma^2[m] = \frac{N}{kT}\left[\langle m^2 \rangle - \langle m \rangle^2\right],\tag{62}$$

  the internal energy per spin, $u = U/N$, given by

$$u = \frac{\langle H \rangle}{N},\tag{63}$$

and the specific heat per spin, $c = C/N$, which can be related to the fluctuations of energy

$$c = \frac{\sigma^2[H]}{kT^2N} = \frac{1}{kT^2N} \left[\langle H^2 \rangle - \langle H \rangle^2 \right] , \tag{64}$$

and many others.

- Relations between a response function (χ_T, c, ...) and microscopic fluctuations ($\sigma^2[m]$, $\sigma^2[H]$, ...) were first obtained by Einstein and go under the general name of fluctuation-dissipation relations.

- The idea is then to replace true averages by sample averages. For instance, for the magnetization, we will write

$$\langle m \rangle = \frac{1}{M} \sum_{k=1}^{M} m_k , \tag{65}$$

where m_k is the value of the magnetization computed in $k = 1, \ldots, M$ spin configurations $\boldsymbol{s}_1, \ldots, \boldsymbol{s}_M$. Remember that each configuration $\boldsymbol{s}$ is a set of values for the N spin variables $\boldsymbol{s} = (s_1, \ldots, s_N)$. The configurations $\boldsymbol{s}_k$ must be generated according to the probability

$$f(\boldsymbol{s}) = Z^{-1} \mathrm{e}^{-\beta H(\boldsymbol{s})} . \tag{66}$$

- We consider now the Metropolis algorithm to generate the configurations $\boldsymbol{s}_k$. The basic ingredient is the proposal probability $g(\boldsymbol{s}'|\boldsymbol{s})$. We should not be surprised now of the general strategy: the proposed configuration $\boldsymbol{s}'$ differs from $\boldsymbol{s}$ only in the value of a *single spin variable*. Therefore, we select a site, say i, and propose a change $s_i \to s_i'$. It should be clear that the only possible proposal is $s_i' = -s_i$, that is, to propose $s_i' = \pm 1$ if $s_i = \mp 1$.

- What is the change in the Hamiltonian $\Delta H = H(\boldsymbol{s}') - H(\boldsymbol{s})$ associated with this proposal? As $N - 1$ spins remain unchanged, the only variation in the Hamiltonian comes from the terms of the sum in H in which the

selected spin s_i appears. Let us denote by $s_{i_1}, \ldots, s_{i_z}$ the set of neighbors of s_i. Therefore, the change is

$$\Delta H = \left(-J \sum_{\mu=1}^{z} s_i' s_{i_\mu} - h s_i'\right) - \left(-J \sum_{\mu=1}^{z} s_i s_{i_\mu} - h s_i\right) = 2 s_i \left(J \sum_{\mu=1}^{z} s_{i_\mu} + h\right), \tag{67}$$

where we have used that $s_i' = -s_i$ in the last step.

- The acceptance probability can be chosen as $h(\boldsymbol{s}'|\boldsymbol{s}) = \min[1, \mathrm{e}^{-\beta \Delta H}]$, the Metropolis rate, or $h(\boldsymbol{s}'|\boldsymbol{s}) = (1 + \mathrm{e}^{+\beta \Delta H})^{-1}$, the Glauber rate, or any other convenient expression.

- Let us now give some details of the programming in the case of a regular $2d$ square lattice. Most of what we will say can be straightforwardly extended to other lattices, regular or random.

- The first thing we need to do is to store the configuration $(s_1, \ldots, s_N)$. As the variables are ± 1, it is possible to use very sophisticated storage methods where each variable occupies only one bit of memory (a bit equal to 0 corresponds to $s_i = -1$ and a bit equal to 1 to $s_i = +1$). However, we start by a simple storage method in which spin s_i is stored in location $s(i)$ of an array of integers. We then define `integer s(N)` as the array where we store the variables.

- As we are in a square lattice, the number of sites is $N = L^2$, and we could as well store the variables in a two-index array, such as `integer s(L,L)`. Both notations are equivalent (Figure 4). However, the use of a single index brings many simplifications to the program structure and we will keep this way of storing the variables. It is convenient to keep in mind that if we use Cartesian coordinates (i_x, i_y), $i_x, i_y = 1, \ldots, L$, the single index $i = 1, \ldots, N$ is given by $i = (i_y - 1) \times L + i_x$.

- In the square lattice, spin s_i has $z = 4$ neighbors which we name $s_{i_1}, s_{i_2}, s_{i_3}, s_{i_4}$. These neighbors are located, respectively, at the right, top, left, and bottom sites of i (Figure 1). It is convenient, instead of computing every time the indexes i_1, i_2, i_3, i_4 that correspond to site i, to store those values on arrays, such that they can be
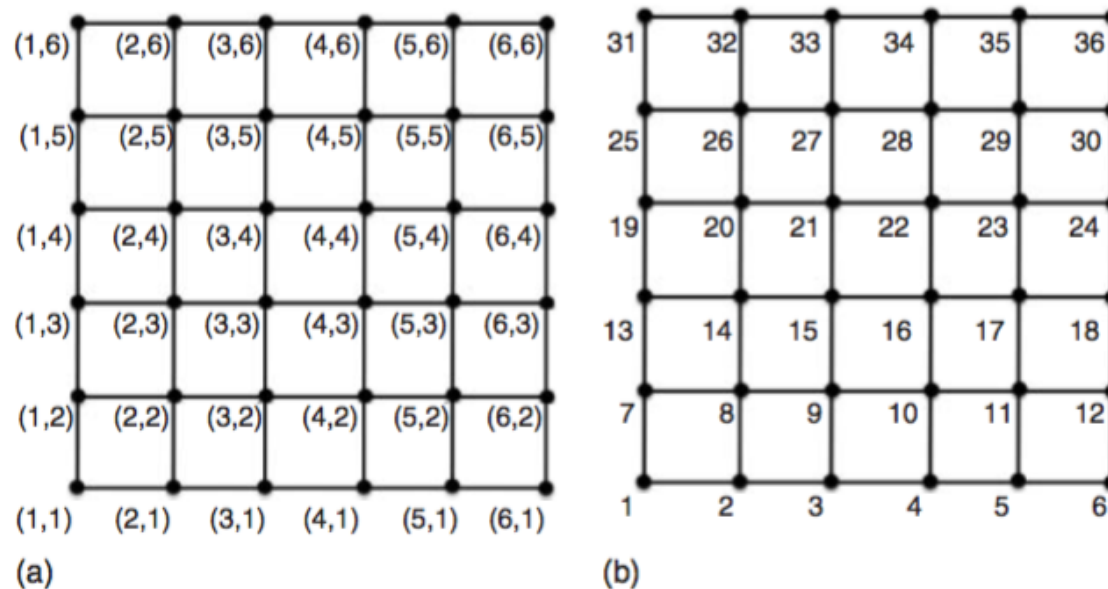
Figure 4. Storage of the nodes of a square lattice using (a) two indexes (i_x, i_y) or (b) a single index i. The figure exemplifies these two possibilities in the case of a linear side $L = 6$.

easily (i.e. quickly) accessed when needed. We use the array integer n1(N) such that the value n1(i) is equal to i_1, the right neighbor of site i. Similarly, the arrays integer n2(N), n3(N), n4(N) store the locations of the up (i_2), left (i_3), and down (i_4) neighbors of site i.

• Boundary conditions: A case of special interest is the spins at the borders of the square lattice. One might simply consider that the spins at these borders do not have as many neighbors as the others. A more commonly used choice is that of periodic boundary conditions, or pbcs for short. This means that the right neighbor of a site which is located at the right edge of the square is located in the same row at the left edge: and similarly for other directions. Figure 5 sketches the nearest neighbor connectivity in the square lattice. It is as if the right and left edges, and the top and the bottom ones, are connected. The resulting closed structure has torus topology.
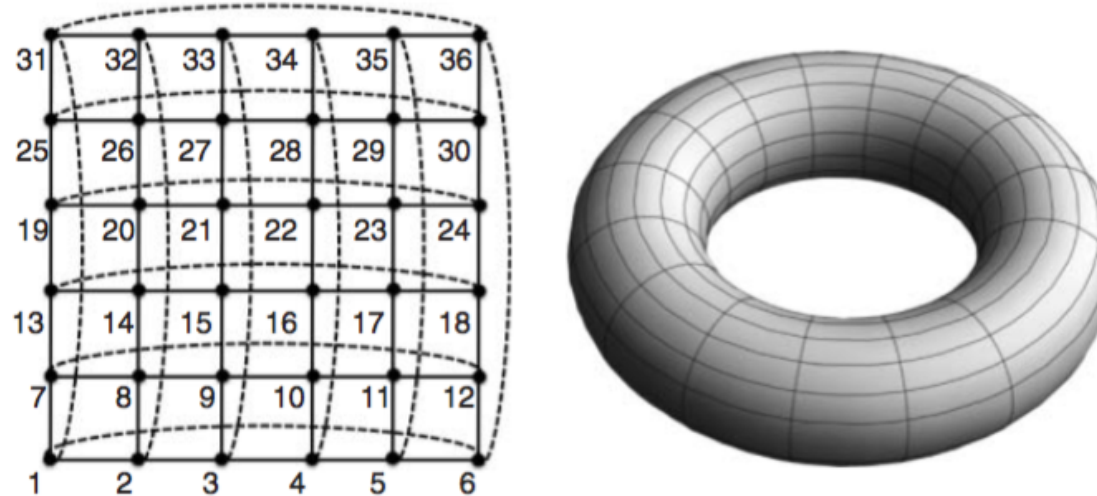
Figure 5. Nearest neighbor connectivity in a square lattice using periodic boundary conditions and the resulting torus topology. For example, the nearest neighbors of site $i = 12$ are $i_1 = 7$, $i_2 = 18$, $i_3 = 11$, and $i_4 = 6$, while the nearest neighbors of site $i = 31$ are $i_1 = 32$, $i_2 = 1$, $i_3 = 36$, and $i_4 = 25$.

- In order to generate the right values for those arrays, we use the `subroutine neighbors`. It uses conveniently the equivalence between the one-index i and the two-index (i_x, i_y) notations to find the four neighbors of a site. This routine implements the pbcs. For example, the right neighbor of site $(i_x = L, i_y)$ is not $(L + 1, i_y)$ but $(1, i_y)$, and so on.

```fortran
! Subroutine to compute and save the nearest neighbors of a
! 2d square-lattice Ising model under periodic boundary conditions
subroutine neighbors(n1,n2,n3,n4,L)
dimension n1(L*L),n2(L*L),n3(L*L),n4(L*L)
do ix=1,L
   do iy=1,L
      i=(iy-1)*L+ix
      ix1=ix+1
      if (ix1.eq.L+1) ix1=1
      n1(i)=(iy-1)*L+ix1

      iy2=iy+1
      if (iy2.eq.L+1) iy2=1
      n2(i)=(iy2-1)*L+ix

      ix3=ix-1
      if (ix3.eq.0) ix3=L
      n3(i)=(iy-1)*L+ix3

      iy4=iy-1
      if (iy4.eq.0) iy4=L
      n4(i)=(iy4-1)*L+ix
   enddo
enddo
end subroutine neighbors
```

- Next thing to consider is the calculation of the acceptance factor. The possible change of energy in the case a magnetic field $h = 0$ can take only five possible values, namely

$$- \beta \Delta H = -2\beta J s_i \sum_{\mu=1}^{z} s_{i_\mu} = -2KB_i = -2K \begin{cases} -4 \\ -2 \\ 0 \\ +2 \\ +4 \end{cases}$$

  where we have defined $K = \beta J$ and $B_i = s_i \sum_{\mu=1}^{z} s_{i_\mu}$, being the sum of four numbers, each one being ± 1, can only take the values indicated above. Similarly, the Boltzmann-Gibbs factor

$$\mathrm{e}^{-\beta \Delta H} = \mathrm{e}^{-2KB_i} \tag{68}$$

  can only take five possible values.

- We decide to store the acceptance probabilities in the array `h(-4:4)`. This is defined as

$$\texttt{h(j)} = \min[1, \mathrm{e}^{-2Kj}], \qquad j = -4, -2, 0, +2, +4. \tag{69}$$

  To accept, we compare `h(j)` with a homogeneous random number u in the usual way. If $u < $ `h(j)`, we accept the proposal. Otherwise, it is discarded and we must make a new proposal by selecting randomly another spin variable.

- All the preliminary steps are now defined. The program, after creating the arrays of neighbors and setting the initial condition randomly assigning values $s_i = +1$ and $s_i = -1$ with probability $1/2$, then performs the proposal/acceptance steps. These are divided into two blocks: first, we perform `M0*N` thermalization steps, which is equivalent to `M0` Monte Carlo steps (MCSs) (one MCS is equal to N basic proposal/acceptance steps);

next, we begin the `M` measurements. Before each measurement, we perform `mc*N` updates, or `mc` MCS. In this simple implementation, we measure three things: the magnetization $\langle m \rangle$ (stored in `rm`), its fluctuations $\langle m^2 \rangle - \langle m \rangle^2$ (stored in `rm2`), and the correlation function $\rho_m(t = \texttt{mc}\ \text{MCS})$, or the correlation between two consecutive values of the magnetization (stored in `c`).

- Finally, the program runs for different values of temperature. In a setup like this, it is convenient to start first at a high value of the temperature ($T = 4$ in the listing below), where the thermalization times are smaller. When lowering the temperature, we do not generate again the initial condition, but use instead the final configuration at the previous, higher, temperature.

- We now provide a full program

```
! Monte Carlo simulation of the 2d square-lattice Ising model
! under periodic boundary conditions
program Ising_2D_Metropolis

parameter (L=80,N=L*L)
implicit double precision(a-h,o-z)
integer s(N),n1(N),n2(N),n3(N),n4(N)
dimension h(-4:4)
data M,M0,mc /8192,1000,1/

! We first generate the different neighbor vectors
call neighbors(n1,n2,n3,n4,L)
```

```fortran
! Random initial configuration
do i=1,N
    if (ran_u() < 0.5d0) then
        s(i)=+1
    else
        s(i)=-1
    endif
enddo
! Loop over temperatures
do 999 T=4.0,0.1,-0.1
! For each T, create array with Boltzmann-Gibbs factors
    do j=-4,4,2
        h(j)=min(1.0,exp(-2*j/T))
    enddo
! Thermalization (relaxation to steady state)
    do  ij=1,M0*N
        i=i_ran(N)
        ib=s(i)*(s(n1(i))+s(n2(i))+s(n3(i))+s(n4(i)))
        if (ran_u() < h(ib)) s(i)=-s(i)
    enddo
! Initialize averages
    c=0.0           ! Average correlation
    rm=0.0           ! Average magnetization
    rm2=0.0           ! Average magnetization**2
    rm1=real(abs(sum(s)))/N
```

```fortran
! Updating steps
   do  im=1,M
      do ij=1,mc*N
         i=i_ran(N)
         ib=s(i)*(s(n1(i))+s(n2(i))+s(n3(i))+s(n4(i)))
         if (ran_u() < h(ib)) s(i)=-s(i)
      enddo
! Begin measurements
      rm0=real(abs(sum(s)))/N   ! Current abs(magnetization)
      write(88,*) rm0
      rm=rm+rm0
      rm2=rm2+rm0*rm0
      c=c+rm0*rm1
      rm1=rm0
   enddo
! Final averages
   rm=rm/M
   rm2=rm2/M-rm*rm
   c=(c/M-rm*rm)/rm2
   if (c.ne.1.0) tau=c/(1.0d0-c)
   error=sqrt(rm2*(2*tau+1)/M)
   write(66,'(f10.6,1p5e16.6)') T,rm,rm2,error,mc*tau,c
999 continue
end program  Ising_2D_Metropolis
```
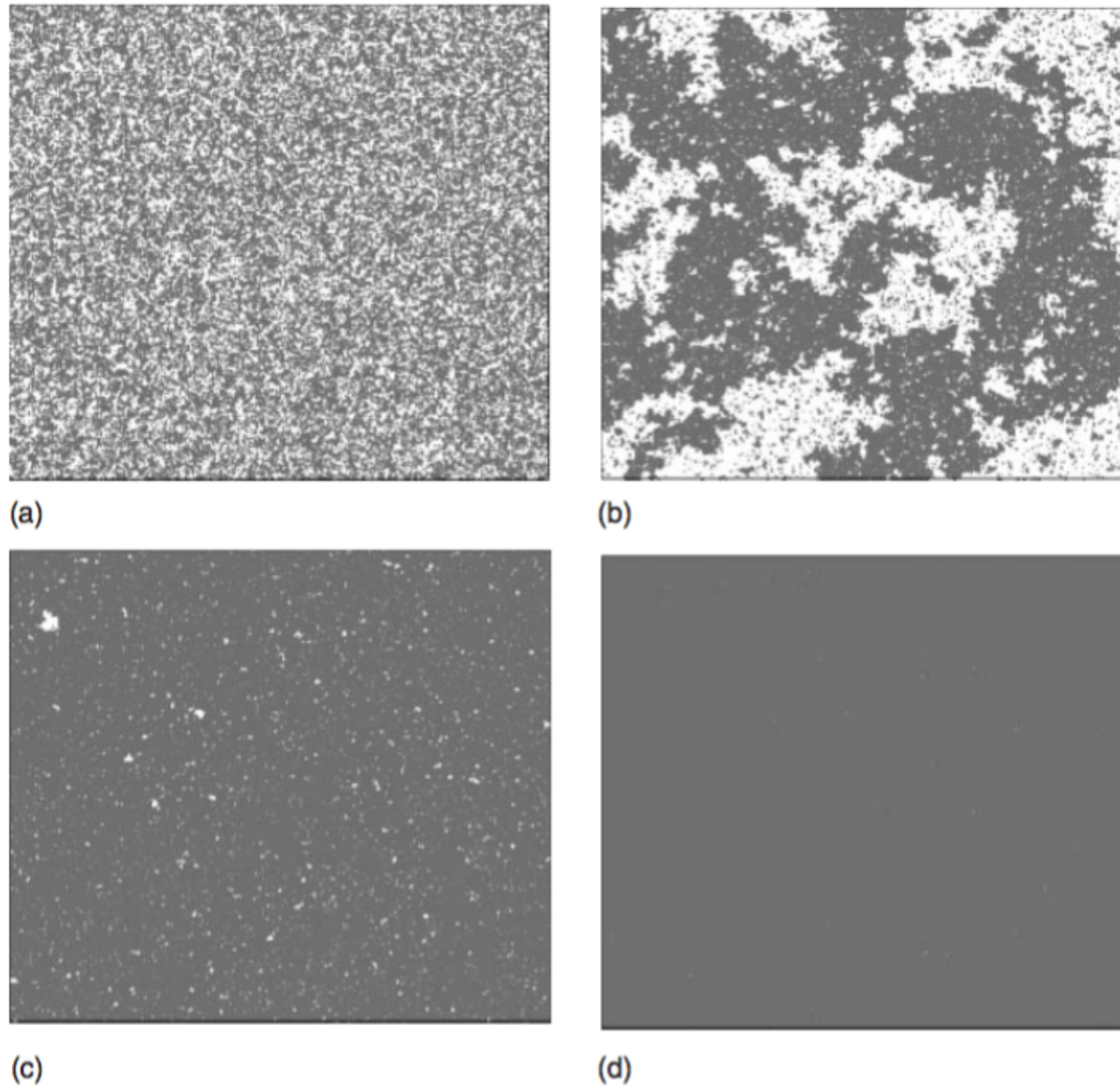
Figure 6. Representative configurations of the Ising model at (a) $T = 4$, (b) $T = T_c$, (c) $T = 2$, and (d) $T = 1$, for a system of $N = 4002$ sites. A spin up, $s_i = +1$, is indicated by a dark dot, whereas a spin down, $s_i = -1$, is represented by a white dot. Observe that, at $T = T_c$, the structure is fractal, meaning that there are many blocks of up spins in a background of down spins, and vice versa, recursively.

- In Figure 6, we plot some representative configurations obtained after running this basic Ising model program. We can see the order–disorder phenomenology: at temperatures larger than the critical temperature T_c, the system is disordered and there is, on a local average, approximately the same number of up and down spins. At low temperatures, one of the two spin options dominates (symmetry breaking). At $T \approx T_c$, there is still the same average number of up and down spins, but they begin to organize themselves in a fractal-like self-similar structure, the precursor of the phase transition.

6. Binary alloys, lattice gases and Kawasaki interpretation of the Ising model

- The Ising model can be used in very many different contexts. An interesting interpretation as a model for binary alloy separation was introduced by Kawasaki.

- In his model, a variable taking a value $s_i = +1$ indicates that on node i there is one atom, A, of a particular metal (e.g., aluminum), whereas $s_i = -1$ indicates the presence of another type of atom B (e.g., zinc).

- The Hamiltonian is still given by

$$H(s_1, \ldots, s_N) = -J \sum_{\langle i,j \rangle} s_i \, s_j - h \sum_i s_i \,, \tag{70}$$

  but now the magnetic field h is interpreted as the difference in chemical potential between the two types of atoms.

- The novelty compared to the usual interpretation as a ferromagnet is that atoms A and B cannot transmute. This means that the number of A atoms and the number of B atoms are both constant and conserved by the dynamics. The averages have to be performed with respect to the same pdf as before, $f(\boldsymbol{s}) = Z^{-1}e^{-\beta H(\boldsymbol{s})}$, but only the total number of A atoms is a prefixed number N_A (and consequently the number of B atoms is $N_B = N - N_A$).

- How do we implement such a constraint in our proposal probability $g(\boldsymbol{s}'|\boldsymbol{s})$? Kawasaki's proposal is to allow for changes $\boldsymbol{s} \to \boldsymbol{s}'$ by which two neighboring atoms *exchange positions*. This certainly keeps both the number of A and B atoms constant; they simply move around. It is also required to mimic the real diffusion process that occurs in an alloy as it is cooled down from a high-temperature phase.

- Therefore, in the proposal step we select a pair of neighbor sites i, j, check that $s_i = -s_j$ (otherwise, it does not matter whether we accept the change or not), and propose the change $(s_i, s_j) \to (s'_i, s'_j)$ with $s'_i = s_j = -s_i$, $s'_j = s_i = -s_j$. It is clear that this is a symmetric proposal, $g(\boldsymbol{s}'|\boldsymbol{s}) = g(\boldsymbol{s}|\boldsymbol{s}')$.

- In order to choose the pair of neighboring sites, we first choose i randomly between 1 and N. Then, in the square lattice, it suffices to select j with equal probability as the neighbor to the right or the neighbor at the top. Work out the details!

- Regarding the order parameter, of course now it does not make sense to compute the average magnetization, as this is a constant (it is the number of A atoms minus the number of B atoms). A typical quantity to measure instead is the number of links that join two nearest neighbor sites in which the variables take different values, a sort of contact area between the metals of the two alloys.

- One of the most important drawbacks of this algorithm is that it might occur too often that the two selected sites hold the same type of atoms, and then this trial has to be repeated. A possibility is to make a list of all possible pairs of neighboring sites that hold different values for the spin variables and then choose a pair only from this list. This possibility speeds up the program but it does require some amount of programming[1]

- Considered as a real model for a binary alloy, the Kawasaki model is able to reproduce some well-known facts known to metallurgists. First, the process leads to phase separation (with each alloy occupying mainly a localized spatial area) only below a critical temperature, T_c. For $T > T_c$, the two metals are well mixed, whereas for $T < T_c$ the system splits into two phases, each one of them rich in one of the metals. The second interesting feature of the Kawasaki model is that the time evolution of the phase separation process occurring at temperatures below T_c depends strongly on the initial relative proportion of each metal. If this proportion is close to 50%, then the process proceeds by what is called spinodal decomposition in which filament-like structures linking all the atoms of one metal begin to form and then coarsen and grow. When one of the metals is more abundant than the other, droplet nucleation and growth is observed: the metal that is in minority starts forming small droplets embedded in the majority metal. These droplets then begin to coalescence and form larger droplets, until only

† This modification constitutes the *n-fold way* proposed by Bortz, Kalos, and Lebowitz.
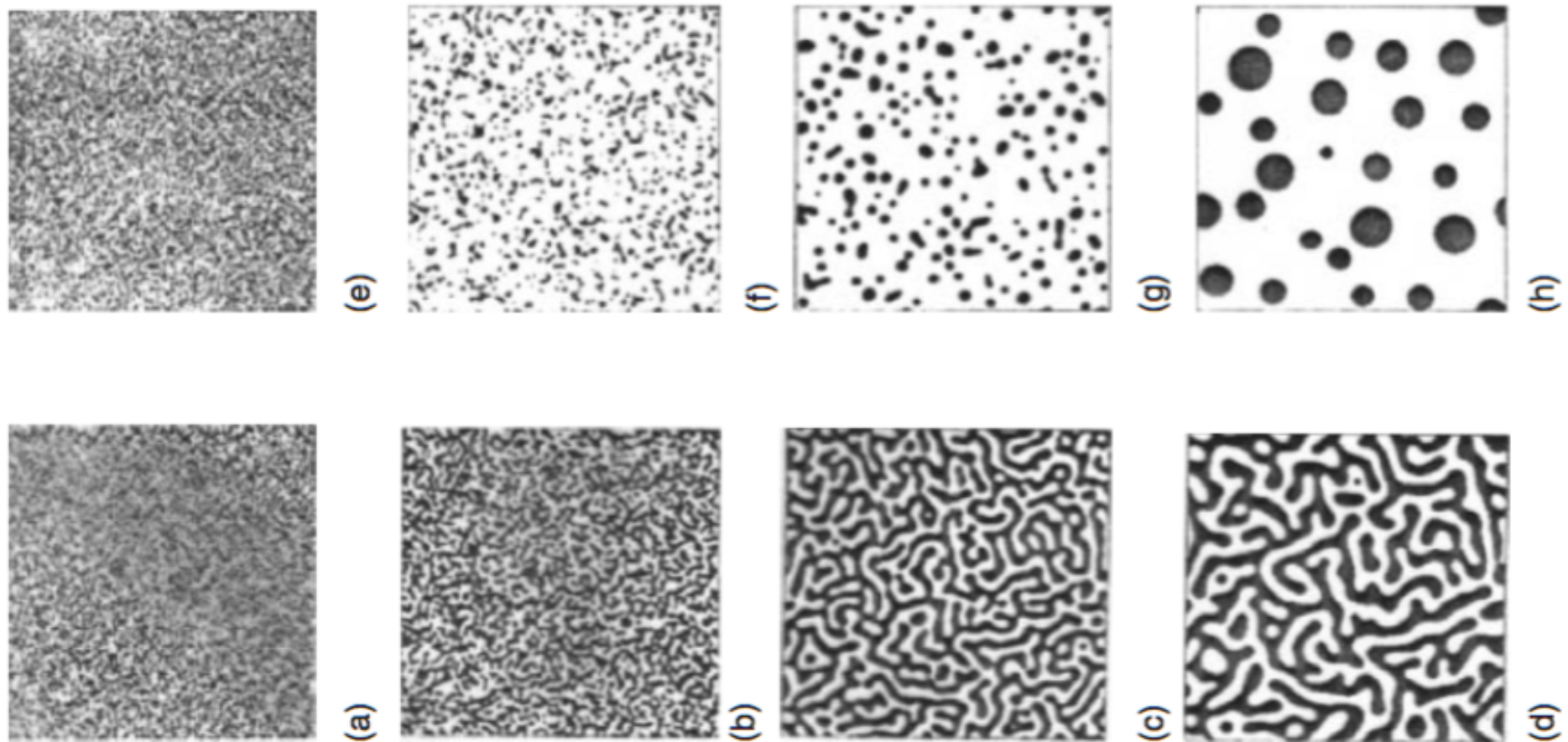
Figure 7. Representative configurations of the Kawasaki version of the Ising model at $T = 0.95$ starting from an initial condition with exactly half the spins in the +1 state (a–d), and starting with one-third of the spins in the +1 state (e–h). In both cases, time runs from left to right. In (a–d), we see the *spinodal decomposition* evolution mechanism, whereas in (e–h) we observe the *nucleation and growth of droplets* of one phase.

one big one (and maybe several very minor droplets) can be seen. These different evolution processes can be observed in Figure 7.

- Note also that the Kawasaki version of the Ising model can be interpreted as a model of a (lattice) gas. In this interpretation, particles correspond to $s_i = +1$ and holes to $s_i = -1$. Equivalently we can work with occupation variables $n_i = (1 + s_i)/2$, such that a particle (hole) corresponds to $n_i = 1(0)$. This model hence allows to investigate in detail the gas–liquid phase transition which appears in most fluids as temperature is varied. Not surprisingly, this phase transition belongs in the *Ising universality class*.

7. Data analysis: Caveats around the critical region

- Once we have developed our Monte Carlo code for the Ising model above, the next logical step is to run it and to obtain some results of interest. However, this process is not without danger.

- In Fig. 9 we plot the spontaneous magnetization (at zero magnetic field) of the Ising model as obtained from our program for three different system sizes: $L = 20, 40$, and 80, as well as the exact solution given by Onsager, see Eq. (59).

- From this figure, we notice clearly two things: (i) for a considerable range of temperatures, the numerical plots are well outside the theoretical result, and (ii) the error bars are not constant for all values of the temperature, but they are considerable larger near the critical region.

- The first discrepancy is due to finite-size effects. Concerning the magnitude of the error bars, we recall that the error in the sample average of the magnetization can be written as

$$\varepsilon[m] = \frac{\sigma[m]}{\sqrt{M}} \sqrt{2\tau_m + 1} \,, \tag{71}$$

where M is the number of points contributing to the sample average, $\sigma^2[m] = \langle m^2 \rangle - \langle m \rangle^2$ is the variance of m, and τ_m is the correlation time associated with the normalized correlation function ρ_m. Certainly, the errors decrease by increasing the number of measurements M, and we can ask which one of the two factors, $\sigma[m]$ or τ_m, is responsible for the observed error increase around the critical region.

- The not-so-encouraging answer is that both factors contribute. Around the critical region one observes (i) an increase of fluctuations $\sigma[m]$, and (ii) an increase of the correlation time τ_m due to the so-called *critical slowing down*.
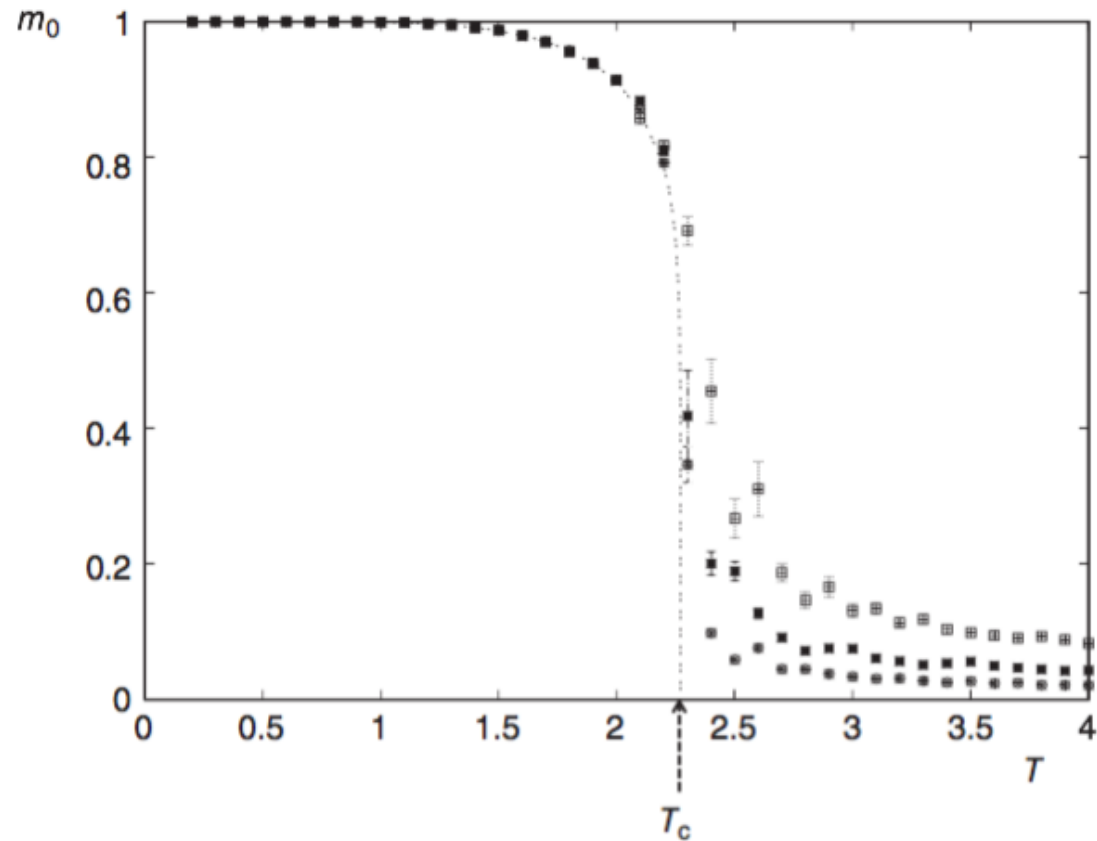
Figure 8. Spontaneous magnetization m_0 of the Ising model in the square lattice as a function of temperature T for different values of the system side $L = 20, 40, 80$ from top to bottom in the right-hand side of the figure. The dots have been obtained using the Metropolis algorithm. The dashed line is Onsager's exact solution, as given by Eq. (59). We have set units such that $k = J = 1$.

- Finite-size effects, increase of fluctuations, critical slowing down, and thermalization are the major points of concern in many Monte Carlo simulations. We now discuss these points separately. These problems are not specific to the Ising model. They can also be observed in the numerical simulations of every other system that we simulate near a phase transition.

7.1. Finite-size effects and scaling

- The discontinuities and mathematical singularities which characterize a true phase transition only appear in the thermodynamic limit $N \to \infty$.

- For instance, Onsager's solution (59) implies a discontinuity of the derivative of $m_0(T)$ at $T = T_c$. In fact, the theory of phase transitions predicts that the asymptotic behavior near the critical point is

$$m_0(T) \sim |1 - T/T_c|^\beta , \qquad \text{for } T \leq T_c , \tag{72}$$

with a value of the *"critical exponent"* $\beta = 1/8$ for the 2d Ising model.

- Similarly, it predicts that the magnetic susceptibility diverges at the critical point as

$$\chi_T \sim |1 - T/T_c|^{-\gamma} \tag{73}$$

with a value of the critical exponent $\gamma = 7/4$, for the 2d Ising model, implying formally that the magnetic susceptibility diverges at $T = T_c$. Moreover, recalling that $\chi_T = \frac{N}{kT}[\langle m^2 \rangle - \langle m \rangle^2]$, the divergence of χ_T at T_c also implies that the variance of the order parameter greatly increases near the critical temperature. These are examples of the typical non-analytical behavior that occurs at the critical point.

- Strictly speaking, however, a non-analytical behavior cannot appear in a finite system[1]. What it is observed in the simulations, though, is a big increase of the susceptibility in the neighborhood of the critical region (Figure

† Think in terms of our simulation. It is impossible that $\chi_T = \frac{N}{kT}[\langle m^2 \rangle - \langle m \rangle^2]$ is equal to ∞ anywhere as the fluctuations of the order parameter are bounded, $|m| < 1$, and we never divide by 0.
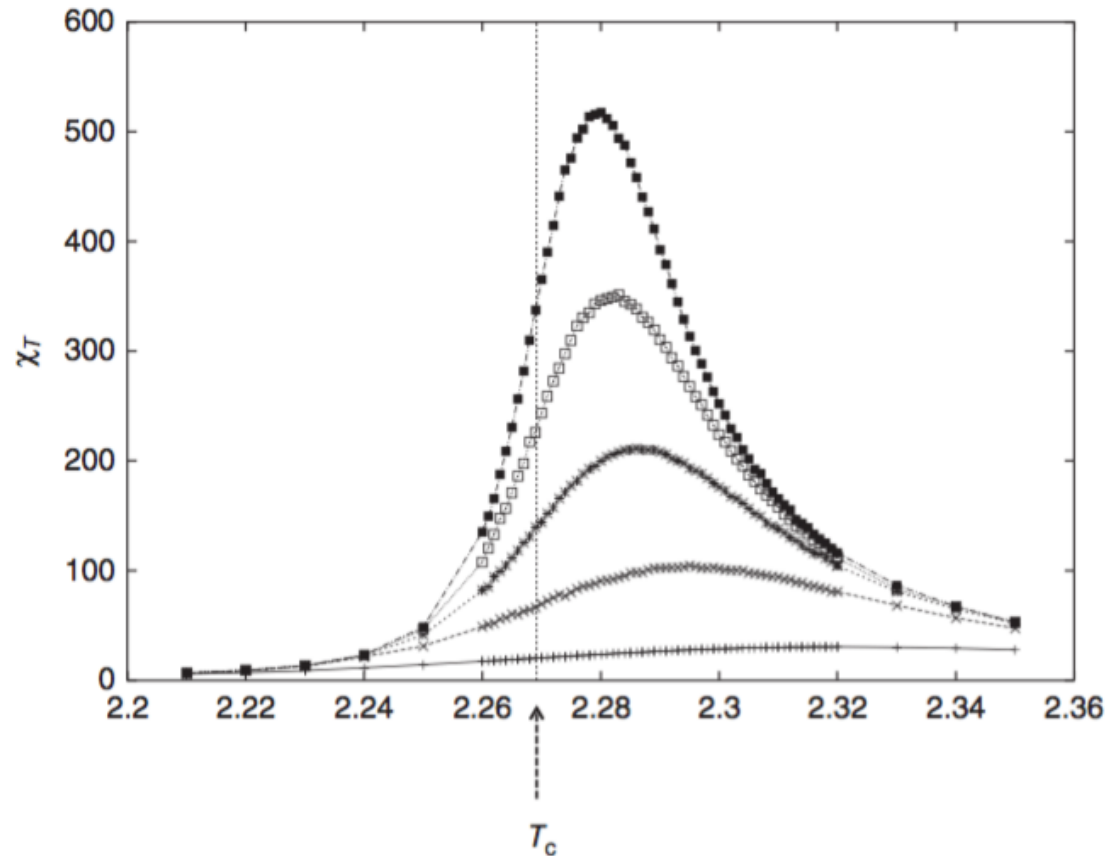
Figure 9. Magnetic susceptibility χ_T for the $2d$ square Ising model computed using the Metropolis algorithm for system sides $L = 40, 80, 120, 160, 200$. The maximum value increases for increasing L.

9). As the system size N increases, the maximum in the susceptibility grows higher and its location approaches the true critical temperature T_c of the infinite system.

- The importance of finite-size effects near a second-order phase transition can be understood intuitively. In this situation, the correlation length, which measures the linear range over which spins at different sites of the lattice

are correlated, diverges (in an infinite system) with a power-law singularity

$$\xi(T) \sim |1 - T/T_c|^{-\nu}, \tag{74}$$

where $\nu = 1$ for the $2d$ Ising model. For a finite system, the correlations cannot extend beyond the system side and we must have $\xi \sim L$. The theory of finite size effects tells us exactly how (and why!) the averages of interest behave.

- The basic idea is that now the magnetization becomes a *homogeneous function* of ξ and the system side L, that is, $m(\xi, L) = \xi^x \tilde{m}(\xi/L)$. The unknown exponent x is obtained by demanding that in the infinite system, and close enough to the critical point, one recovers the known behavior $m_0(T) \sim |1 - T/T_c|^{\beta}$. This implies that the function $\tilde{m}(z)$ takes a finite limit when $z \to 0$, and then

$$m_0(T) = \lim_{L \to \infty} m(T, L) = \xi^x \tilde{m}(0) \sim \left[|1 - T/T_c|^{-\nu}\right]^x \sim |1 - T/T_c|^{-x\nu} \sim |1 - T/T_c|^{\beta}, \tag{75}$$
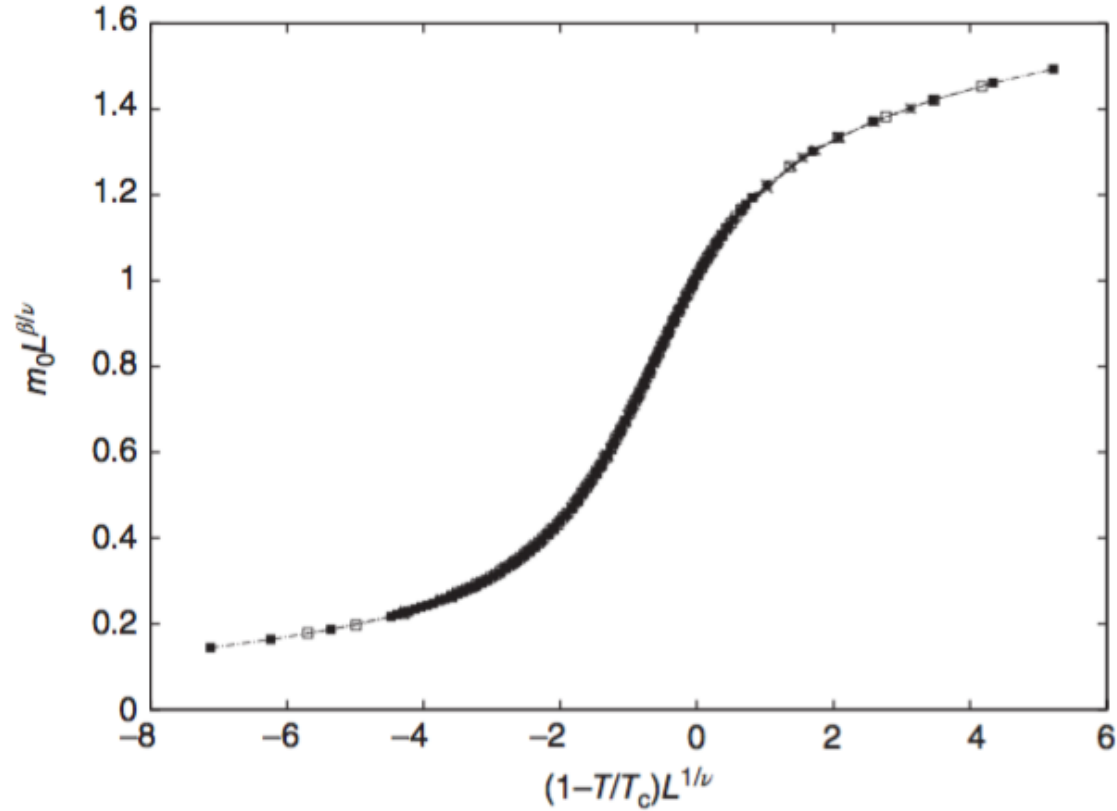
and therefore $\beta = -x\nu$.

- In this way, the prediction for the magnetization *near the critical point* for a finite system is

$$m_0(T, L) = \xi^{-\beta/\nu} \tilde{m}(\xi/L) = L^{-\beta/\nu} \bar{m}\left[(1 - T/T_c)L^{1/\nu}\right]. \tag{76}$$

- The typical way of checking this scaling behavior is to plot $m_0(T, L)L^{\beta/\nu}$ versus the rescaled variable $(1 - T/T_c)L^{1/\nu}$, see Fig. 10.

- One can use as well the corresponding scaling relations for the specific heat and the susceptibility

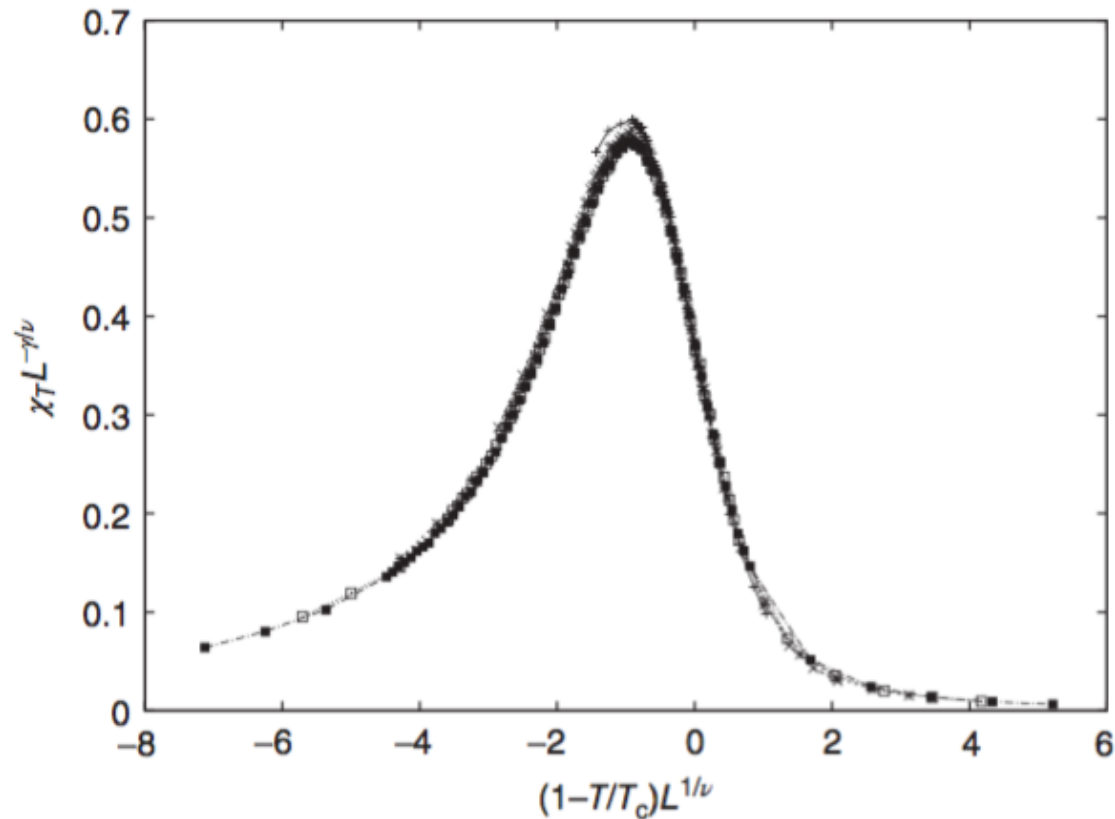$$c(T, L) = L^{\alpha/\nu} \bar{c}\left[(1 - T/T_c)L^{1/\nu}\right] \tag{77}$$

Figure 10. Check of the scaling relation with system size of the magnetization. Data for $L = 40, 80, 120, 160, 200$ have been collapsed onto the same curve using the rescaling of axes as indicated.

and

$$\chi_T(T, L) = L^{\gamma/\nu} \bar{\chi} \left[(1 - T/T_c) L^{1/\nu} \right] \tag{78}$$

The scaling relation for χ_T has been checked in Fig. 11.

- In the previous data collapses we have used the known values for the critical temperature T_c and the critical

Figure 11. Check of the scaling relation with system size of the susceptibility. Data for $L = 40, 80, 120, 160, 200$ have been collapsed onto the same curve using the rescaling of axes as indicated.

exponents ν, β and γ for the 2d Ising model. If, as it is usually the case, the critical temperature and the critical exponents are not known, but their knowledge is the ultimate goal of our simulation, this procedure implies a three-parameter fit which is rather difficult to carry out in practice.

- The fitting has another important problem, namely, that the scaling relations derived above are only valid
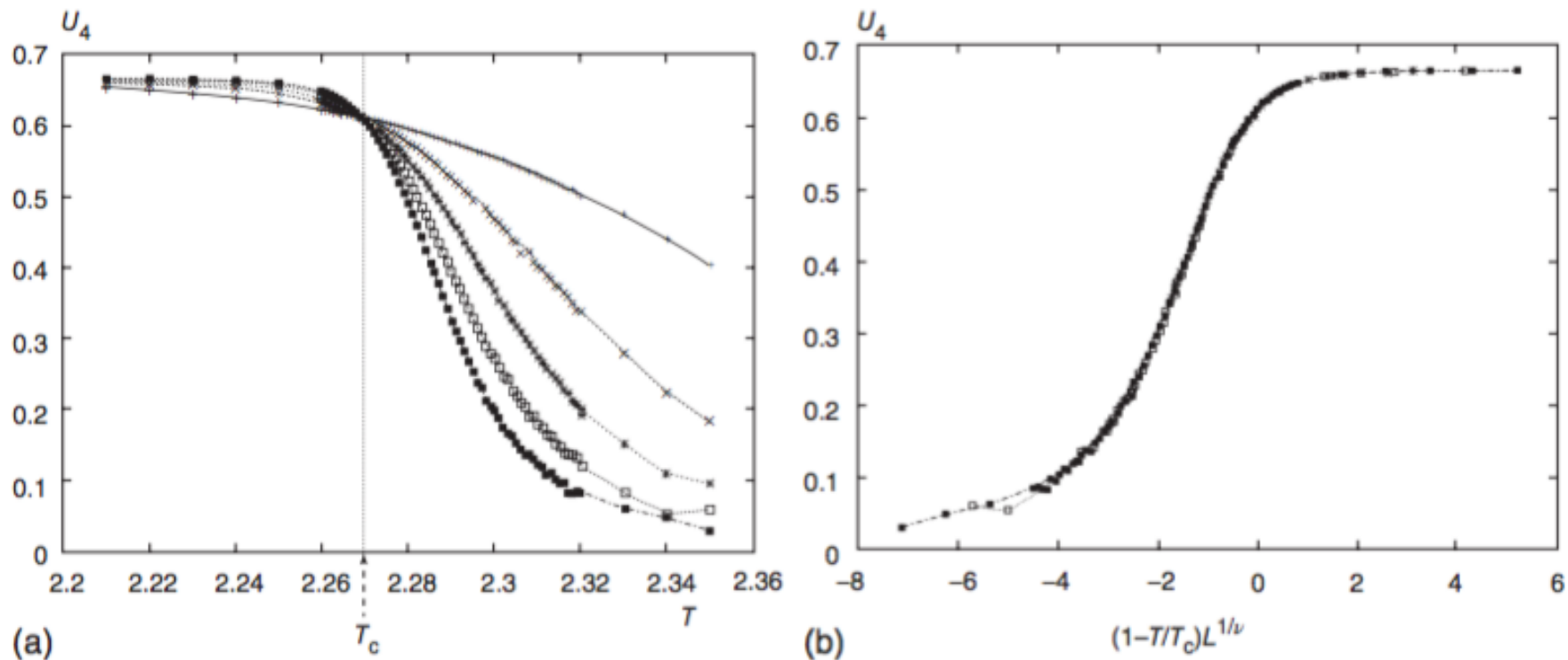
Figure 12. (a) Behavior of the ratio of moments U_4 defined in the text coming from numerical simulations of the $2d$ square Ising model for system sizes $L = 40, 80, 120, 160, 200$. The common crossing of the curves for different values of L indicates the critical temperature T_c. (b) The data have been collapsed onto the same curve using the rescaling of the horizontal axis as indicated.

asymptotically for large L and close enough to T_c. What is meant by *"large L"* and *"sufficiently close to T_c"* is something that cannot be asserted before we do the simulations. If we add on top of all the large errors that occur near the critical region, it is not strange that some disputes appear continuously about the correct values of the critical exponents for different models of interest in the literature.

- Of particular interest for the analysis of the data is the finite-size scaling behavior of the fourth-order cumulant, or Binder ratio[1], defined as the ratio of moments of the magnetization m defined as

$$U_4(T, L) \equiv 1 - \frac{\langle m^4 \rangle}{3 \langle m^2 \rangle^2} = \bar{U}_4 \left[(1 - T/T_c) L^{1/\nu} \right] . \tag{79}$$

  As $U_4(T_c, L) = U_4(0)$, a constant, the critical temperature T_c can be then determined as the *common intersection* of the $U_4(T, L)$ curves for different values of L, see Fig. 12.

- Once T_c has been determined by this procedure, we can use the fits to determine the values of the critical exponent ν and use those values in the analysis of the curves for the magnetization, susceptibility, and so on.

- However, be aware that these are not easy fits and it is essential to have a precise determination of the errors, including those due to the large autocorrelation times at the critical point.

7.2. Increase of fluctuations

- The variance $\sigma^2[m] = \langle m^2 \rangle - \langle m \rangle^2$ measures the fluctuations of m. As we have discussed, the fluctuations increase at the critical region of a phase transition. This result can be obtained from the relation between the fluctuations and some response functions, such as $\chi_T = \frac{N}{kT} \sigma^2[m]$.

- Near a critical point, the isotherm becomes flat and hence some of these derivatives become formally infinite and have, therefore, associated fluctuations of a very large amount. This increase in fluctuations at the critical point is the origin of the so-called critical opalescence that can be observed with the naked eye and constitutes one of the trademarks of critical points.

† Named after Kurt Binder, a german statistical and computational physicist who first introduced this quantity for the numerical analysis of phase transitions.

- However, from the numerical point of view this is a disaster. If the fluctuations (as measured by $\sigma^2[m]$) increase, so does the error $\varepsilon[m]$.

7.3. Critical slowing down

- As well as the fluctuations, the correlation time τ_m also diverges at the critical point! It is known that the real dynamics of a physical system slows down at the critical region (again, a fact that can be observed experimentally).

- However, we are not using here the real (say Hamiltonian) dynamics, but we have introduced (with some arbitrariness) a convenient Markov chain that allows us to generate representative configurations at equilibrium. Does this stochastic dynamics also suffer from critical slowing down? The answer is yes, as shown by the numerical data and supported by a simple calculation.

- We can obtain an exact expression for the value of the correlation function $\rho_G(1)$ after one elementary proposal-acceptance step. Indeed, using the language of the previous chapter

$$\langle G_{n+1}G_n \rangle = \int dx\, dy\, G(x)\, G(y) f_{\hat{\mathbf{x}}_{n+1}, \hat{\mathbf{x}}_n}(x, y) = \int dx\, dy\, G(x)\, G(y) f(x|y)\, f_{\hat{\mathbf{x}}_n}(y)\,. \tag{80}$$

Replacing now $f(x|y) = h(x|y)g(x|y) + \delta(x - y)[1 - \epsilon(y)]$, with $\epsilon(y)$ the average acceptance probability given y, and replacing also $f_{\hat{\mathbf{x}}_n}(y)$ for the stationary distribution $f_{\hat{\mathbf{x}}}(y)$, we obtain the one-time normalized correlation function

$$\rho_G(1) = \frac{\langle G_{n+1}G_n \rangle - \langle G_k \rangle^2}{\sigma^2[G]} = 1 - \frac{1}{\sigma^2[G]} \int dx\, dy\, h(x|y)g(x|y) \left[G(x) - G(y)\right]^2 f_{\hat{\mathbf{x}}}(y)\,. \tag{81}$$

We now combine this exact expression with the approximate expression for the correlation time $\tau_G = \rho_G(1)/[1 - \rho_G(1)]$ to obtain

$$\tau_m \approx \frac{2\sigma^2[m]}{\int dx\, dy\, h(x|y)g(x|y) \left[m(x) - m(y)\right]^2 f_{\hat{\mathbf{x}}}(y)} \tag{82}$$

- Consider, for the sake of clarity, the Metropolis algorithm for the Ising model, and we want to compute the correlation time of the magnetization. We know that the proposal for change $x \to y$ is to reverse the sign of a single spin. This yields a modification of $m(x) - m(y) = \pm 2/N$. After squaring, it can be taken out of the integral and we are left with $\int dx\, dy\, h(x|y) g(x|y)\, f_{\hat{x}}(y)$, which is nothing but the average acceptance probability ϵ. We get finally

$$N^{-1} \tau_m = \frac{N \sigma^2[m]}{2\epsilon} = \frac{kT\, \chi_T}{2\epsilon}\,. \tag{83}$$

- $N^{-1}\tau_m \equiv \tau_m^{MCS}$ is the autocorrelation time in units of updates per spin, or MCS. As the average acceptance probability does not decrease near zero at the critical point, it follows that, within this approximation, the critical behavior of the correlation time τ_m^{MCS} is that of the magnetic susceptibility χ_T. As this diverges at the critical point, it turns out that τ_m^{MCS} diverges as well.

- As explained in the previous section, for a finite system of linear side L, it cannot really diverge to infinity, but it grows as a power of the system side

$$\tau_m^{MCS}(T = T_c) \sim L^z\,. \tag{84}$$

The simple expression above would tell us that $z = \gamma/\nu$, the exponent giving the divergence of the susceptibility with system size.

- Intensive numerical simulations using the Metropolis algorithm suggest that the dynamical critical exponent takes a value $z \approx 2$ for the $2d$ Ising model. As the fluctuations increase at the critical point as $\chi_T \sim L^{\gamma/\nu}$, it turns out that the error at the critical point increases with system size as $\varepsilon[m] \sim L^{(z+\gamma/\nu)/2}$ with $(z + \gamma/\nu)/2 \approx 1.9$. Roughly speaking, for the $2d$ Ising model, the errors in the Metropolis algorithm near the critical point increase by a factor of 4 every time we double the system linear side, if we keep the number of measurements M constant.

- While the divergence of the fluctuations (e.g., susceptibility) near a critical point is intrinsic to the model under study, the divergence of τ_m and other correlation times is a property of the numerical method we use to generate

the representative configurations. Therefore, some Monte Carlo schemes have a smaller correlation time than others. It is then important to compare the different possibilities available and to tune up the parameters of the numerical method, whenever possible, in order to obtain the smallest correlation time.

- As far as the Ising model is concerned, the best algorithms use collective updates in which many spins are changed at once. In this way, it is possible to reduce the critical exponent z to a value close to 0. This, however, requires extreme care in the choice of the proposal and acceptance probabilities.